DEVELOPMENT OF FISH CUPULA INSPIRED MULTI-FLUIDIC SENSOR FOR LIQUID SLOSH DETECTION

MOHD ASHRAF AHMAD, ZULKIFLI MUSA, MOHD ANWAR ZAWAWI, MOHD FALFAZLI MAT JUSOF, MUHAMMAD IKRAM MOHD RASHID, MOHD HELMI SUID, ZAHARUDDIN MOHAMED

RESEARCH VOTE NO:

RDU1703153

Fakulti Teknologi Kejuruteraan Elektrik dan Elektronik

Universiti Malaysia Pahang

Acknowledgement

I would wish to convey my earnest gratitude to a number of people who have taught, helped, stimulated and supported this research project.

Firstly, I would like to express my sincere gratitude to Universiti Malaysia Pahang, especially Research Management Center for giving a large amount of money to execute this project, including the sponsorship during conference using the TPDN and TPLN. I hope that the RMC of UMP can still support our project in the future.

Secondly, I would like to thank all the team members for their expert advice and valuable discussion, especially in performing the algorithm in Matlab and LabVIEW, and developing the experimental rig.

Thirdly, I would like to thank our previous supervisor Professor Dr Zaharuddin Mohamed from UTM for his valuable advice and informative discussion. I have learned a lot of skills and techniques that he has presented to me during this period of project, especially in composing a good technical article. I very appreciate for the time and effort that he spends for me.

Abstract

Liquid slosh in a moving vehicle tank will be hazardous to road users and drivers. Because of sloshing liquid in the tank, it is producing some momentum shift in a moving tank truck. Due to these phenomena the tanker truck will be in imbalance position and cause uncontrolled truck. Therefore, to decrease the number of accidents involving lorry carrying liquid, a liquid sloshing sensor is developed to carefully detect the slosh of the liquid and provide an accurate data to control the liquid slosh. Therefore, the objective of this project is to create a slosh detector that mimics the fish cupula structure is considered to observe the liquid slosh behaviour. Using the accelerometer as a detector device, the wave height reading generated by tank movement can be identified and analyzed. This project uses Arduino UNO as a controller to the entire system, as well as communication between the accelerometer and the LabVIEW. Here, the Arduino can manage the connection between the voltage applied to the remote-control car and the sensor data that capture the slosh generated by the tank's movement. It is clarified that the higher the value of the voltage applied to the remote-control car, the higher the reading of the slosh captured by the accelerometer. In addition, the analysis of the sensor reading with respect to the volume of water in the tank is also shown to identify the suitable volume of water in the tank. Based on the above analysis, in order to produce optimum liquid slosh sensor reading, the suitable input voltage of 5 volt for 4 seconds for ¾ volume of water in the tank. On the other hand, this study also develops the dynamic model of the liquid slosh based on the liquid slosh data from the proposed sensor. Here, the identification of liquid slosh using the Hammerstein model based on Sine Cosine Algorithm (SCA). In contrast to other research works, a piece-wise affine function is considered in a nonlinear function of the Hammerstein model, which is more generalized function. Moreover, a continuous-time transfer function is utilized in the Hammerstein model, which is more suitable to represent a real system. The SCA method is used to

tune both coefficients in the nonlinear function and the transfer function of the Hammerstein model such that the error between the identified output and the real experimental output is minimized. The effectiveness of the proposed framework is assessed in terms of the convergence curve response, output response, and the stability of the identified model through the pole-zero map. The results show that the SCA based method can produce a Hammerstein model that yields identified output response closes to the real experimental slosh output with 80.44 % improvement of sum of quadratic error.

Abstrak

Getaran cecair dalam tangki kenderaan yang bergerak akan menjadi berbahaya kepada pengguna jalan raya dan pemandu. Disebabkan getaran cecair dalam tangki, ia menghasilkan beberapa perubahan momentum dalam trak tangki bergerak. Oleh kerana fenomena ini, lori tangki yang akan berada dalam kedudukan ketidakseimbangan dan menyebabkan lori yang tidak terkawal. Oleh itu, untuk mengurangkan bilangan kemalangan yang melibatkan lori yang membawa cecair, sensor getaran cecair dibangunkan untuk mengesan dengan teliti getaran cecair dan menyediakan data yang tepat untuk mengawal getaran cecair. Oleh itu, objektif projek ini adalah untuk mewujudkan pengesan getaran yang meniru struktur Cupula ikan dianggap memerhatikan tingkah laku getaran cecair. Menggunakan accelerometer sebagai peranti pengesan, bacaan ketinggian gelombang yang dihasilkan oleh pergerakan cecair dalam tangki boleh dikenal pasti dan dianalisis. Projek ini menggunakan Arduino UNO sebagai pengawal kepada seluruh sistem, dan juga komunikasi antara accelerometer dan LabVIEW ini. Di sini, Arduino boleh mengurus hubungan antara voltan yang digunakan untuk kereta kawalan jauh dan data sensor yang menangkap getaran cecair yang dihasilkan oleh pergerakan kereta kebal. Ia menjelaskan bahawa nilai yang lebih tinggi daripada voltan yang digunakan untuk kereta kawalan jauh, bacaan yang lebih tinggi getaran yang dihasilkan oleh accelerometer. Di samping itu, analisis hubungan sensor berkenaan dengan isipadu air di dalam tangki juga ditunjukkan untuk mengenal pasti jumlah yang sesuai air dalam tangki. Berdasarkan analisis di atas, untuk menghasilkan cecair optimum bacaan sensor lumpur cair, sesuai voltan input 5 volt selama 4 saat untuk ¾ isipadu air dalam tangki. Sebaliknya, kajian ini juga membangunkan model dinamik daripada lumpur cair cecair berdasarkan data getaran cecair daripada sensor yang dicadangkan. Di sini, pengenalpastian getaran cecair menggunakan model Hammerstein berdasarkan Sine Kosinus Algoritma (SCA). Berbeza dengan kerja-kerja penyelidikan yang lain, fungsi affine keping sudut adalah dalam fungsi tak linear model Hammerstein, yang lebih umum fungsi. Selain itu, fungsi pemindahan berterusan masa digunakan dalam model Hammerstein, yang lebih sesuai untuk mewakili sistem sebenar. Kaedah SCA digunakan untuk kedua-dua pekali dalam fungsi tak linear dan fungsi pemindahan model Hammerstein itu bahawa ralat di antara output yang dikenal pasti dan output eksperimen sebenar dapat dikurangkan. Keberkesanan rangka kerja yang dicadangkan itu dinilai dari segi sambutan penumpuan keluk, sambutan output, dan kestabilan model yang dikenal pasti melalui peta pole-sifar. Hasil kajian menunjukkan bahawa kaedah

SCA berasaskan boleh menghasilkan satu model Hammerstein bahawa hasil dikenalpasti ditutup balas output ke output lumpur cair eksperimen sebenar dengan peningkatan 80.44% daripada jumlah kesilapan kuadratik.

Table of Content

List of Tables

List of Figures

Chapter 1

Introduction

1.1 Background and Research Motivation

In the era of industrial revolution, liquid transportation has been a vital step in industry such as manufacturing. Commodity Flow Survey in 2007, the US alone, 1200 million tons of dangerous liquids are transported using tank trucks [1], making the transportation method the most popular. However, the reported accidents involving tanker trucks is increasing and should be pay attention to it, as a statistic graph shows in 2011; China reported 416 tanker trucks accidents with 643 deaths [2]. This is because sloshing of fuel and other liquids in moving vehicles may cause instability and undesired dynamics [3].

Accidents involving tanker trucks should be alarming the responsible party to take action because this accident possibly causes more disaster as the tanker's content may spill and cause more damage to the surrounding area. From past investigations that involve tanker truck, most of the accident happens is not cause by the driver but due to the rollover and rear-end crashes. There are many reasons for those accidents but the most common one would be liquid sloshing in partially filled tank. Because of sloshing liquid in the tank, it is producing some momentum shift in a moving tank truck. Due to these phenomena the tanker truck will be in imbalance position and cause uncontrolled truck. Therefore, to decrease the number of accidents involving lorry carrying liquid, a liquid sloshing sensor is developed to carefully detect the slosh of the liquid and provide an accurate data to control the liquid slosh.

So far, there are several sensors that have been used to observe the slosh pattern. In [4], an optical encoder sensor is used to measure the water level elevation. In particular, an assembly of a float, connecting arm and optical encoder mounted on the tank wall is used. Meanwhile, the shape of the liquid surface also can be observed using computer vision sensor. For example, in the study from [5], a camera is mounted parallel to the liquid surface and perpendicular to the direction of the tank movement. Here, the liquid is dyed

with red color to increase the contrast to the tank surface. Then, the camera is used to record 25 images per second. A similar technique has been applied in [6], [7] with a video sampling period and image resolution of 16.7 ms and 0.5 mm, respectively. Moreover, other type of sensors for slosh measurement has also been studied in [5], such as capacitive, ultrasonic and infrared based measurements. However, these sensors are generally less sensitive to a rapid oscillation of liquid surface. As shown on the above, most of the sensor developments only consider one degree of freedom (DOF) motion of liquid slosh, which does not accurately consider the chaotic nature of slosh and the complex fluid dynamic in the container. Therefore, a more precise sensor that naturally observes the slosh pattern is required. On the other hand, a microfluidic sensor inspired from fish cupula would provide us a promising mechanism for slosh detection. This is because this kind of sensor has been proved to work effectively in measuring multiple directions of liquid flow [8], [9]. However, it is not clear whether it works for liquid slosh measurement, since there are few literatures to discuss the application of fluidic inspired cupula sensor to the slosh problem. This study aims to investigate the characteristics of the multi-fluidic inspired cupula sensor for liquid slosh measurement. The proposed sensor will be attached to several locations on the tank wall. In particular, the dome-shaped membrane part will be placed slightly under the liquid surface, while the air pressure sensor part will be placed on top of the tank. Both parts will be connected to a micro-tube to transfer the air pressure. A bang-bang torque input will be used to drive the DC motor, which consequently moves the tank and generates the liquid slosh. Moreover, the characteristic of the proposed sensor will be analyzed in terms of minimum level and resolution of liquid displacement, operating air pressure in the membrane, and statistical analysis of liquid oscillation frequency for each fluidic sensor in different locations. Finally, the behavior of the liquid slosh is characterized by nonlinear dynamic model.

1.2 Research Objectives

The objective of this project is given as follows:

(i) To develop a novel multi-fluidic sensor inspired fish cupula for liquid slosh measurement.

(ii) To analyze the characteristic of the proposed sensor in terms of the suitable volume of water in the container, operating conditions of input voltage and optimum location of the proposed sensor.

(iii) To develop the liquid slosh model based on the continuous-time Hammerstein model by using the output data from the proposed sensor.

1.3 Scope of Project

In this study, a mobile liquid slosh plant is considered to replicate real situation of a moving container carrying liquid, as shown in Figure 1.1. In particular, a remote-control car is used to carry a small tank filled with liquid. The tank is also equipped with four plastic wheels so that it can move smoothly as shown in Figure 1.1(a). Moreover, three accelerometer sensors (ADXL335) that are floated on the surface of liquid are used to measure liquid oscillation as shown in Figure 1.1(b). For simplicity of our study, the liquid slosh data from only one of the sensors is recorded and only z-axis output data is considered. Furthermore, the characteristic of the proposed sensor will be analyzed in terms of minimum level and resolution of liquid displacement and statistical analysis of liquid oscillation frequency for each fluidic sensor in different locations. Finally, the behavior of the liquid slosh is characterized by nonlinear dynamic model. Here, the Matlab and Lab view software were used in the simulation and experimental works.

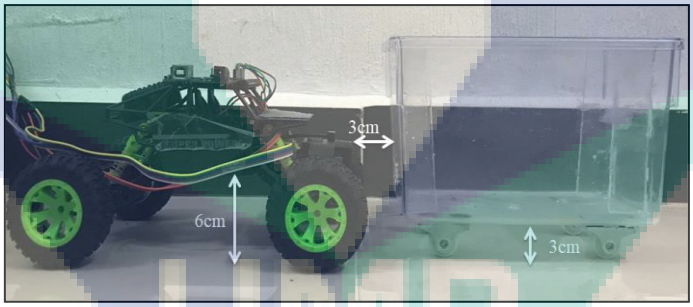

(a) Side view

(b) Plan view

Figure 1.1: Liquid slosh experimental rig

1.4 Organization of Report

This report is organized as follows.

Chapter 2 describes a literature survey on recent sensors in detecting the liquid slosh. These include the capacitive sensor, level sensor and pressure sensor. In addition, we also highlight the motivation of using floating accelerometer to replicate the fish cupula structure. Moreover, a survey on several techniques to model the liquid slosh is also observed.

In Chapter 3, a general framework of designing the sensor platform is explained. A step-by-step procedure of the project process is shown. This is followed by description of several components, circuit diagram, and communication block diagram. Then, we show assemble all the components including sensor with the Lab view platform. In the next sub section, the problem formulation of identifying the liquid slosh model is shown. The step by step procedure of the selected algorithm to find the optimal liquid slosh model based on the sensor data in the previous section is explained.

Chapter 4 presents a performance analysis of the designed sensor to detect the liquid slosh. Their performances are evaluated in terms of minimum level and resolution of liquid displacement and statistical analysis of liquid oscillation frequency for each fluidic sensor in different locations Furthermore, the analysis of the developed liquid slosh model is also presented in terms of integral square error as compared to the real liquid slosh data from sensor.

Chapter 5 concludes this report.

Chapter 2

Literature Review

2.1 Sloshing of Liquids in Partially Filled Tanks

The slosh measurement is crucial for modelling of the slosh phenomenon and for performance evaluation of the designed acceleration cite. Ultimately, one would like a measurement of the Earth's control surface shape and the velocity within the fluid. This is, however, not possible today. The most important measure in this diligence is the surface elevation at the walls of the container. The largest oscillations appear there and one of the control constraints is that the surface does not reach a certain spirit level on the wall. The measurement problem turned out to be nontrivial.

In the most experiment that carry out by the researchers to observe the slosh behaviour is make a setup of the experiment by connect the container to the shaking table that can be move driven by a motor. The displacement of the liquid surface was captured using video or a laser sensor was recorded in order to compare them with those computed numerically at same condition. In the experiment, few descriptions of sloshing parameter such as container shape, container wall use and the field where the experiment is conduct. For the first parameter is the researcher concern about the container shape.

It can be notice that a few people that used asymmetric shape of the container in their own experiments. This is because; in real life, many liquid transportations now day is using the symmetric shape container. Moreover, the researcher also uses rectangular or cylindrical container it because simple design. Besides that, other parameter that has been concern is about container wall use for the experiment. The container wall can be rigid or flexible type. Many researchers use rigid container wall in their investigation. This is because, container wall also plays importance role in measuring slosh. If the wall is flexible the impact of the liquid to the wall will be reduce and it is difficult to get reading of the slosh. However, the best material for the container wall is rigid type like perspex, acrylic or glass material.

2.2 Reviews on Liquid Slosh Measurement Method

2.2.1 Capacitance Based Measurement

This technique uses the difference in permittivity between water and air to calculate the surface condition. The changing of the capacitor in the capacitance that depends on the permittivity of the surrounding medium is the principles of the capacitor-based measurement. The probe and the tank wall form a capacitor whose capacitance is dependent on the amount of product in the tank as shown in Figure 2.1. An empty tank has a lower capacitance, while a filled tank has a higher capacitance. This method is very good measure of the surface condition when the surface is not oscillating [10]. But when the surface is not in the rest state a small layer of liquid is produce on the capacitor plate. This small layer of liquid slide down much slower than the actual surface of the liquid. This make the reading of the capacitance cannot use to measure surface elevation. This method is really working if it is used to measure the value of maximum slosh.

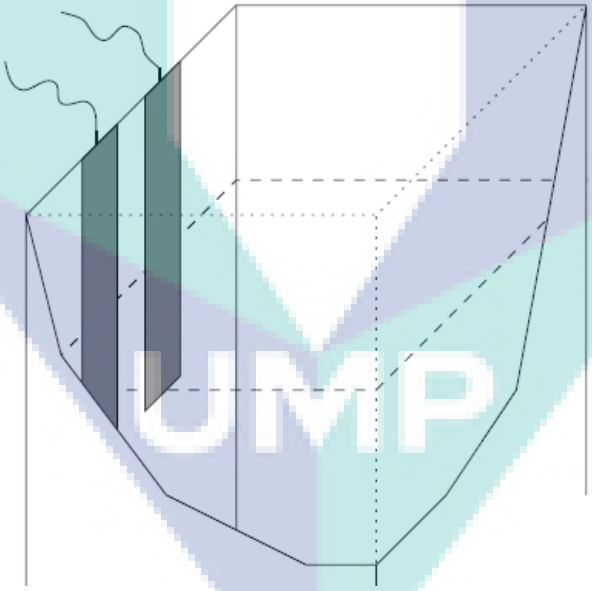

Figure 2.1: Illustration of the capacitance sensor

2.2.2 Pressure Based Measurement

The idea to measure the elevation surface by using the pressure method is to measure the pressure below the actual surface of the liquid as shown in Figure 2.2. To measure using

this method a setup with two aluminum pipes with that have diameter of 6 mm locate at each side of the container. Using plastic tube, the pipe is connected to the pressure sensor.

As the result, this method worked well when the surface is not oscillating, but when the surface was not the in-rest state the value of that measured did not show the actual surface condition [11]. This is because, when the surface of the liquid is not at rest, the pressure does not only depend on the depth but also on the flow velocity.

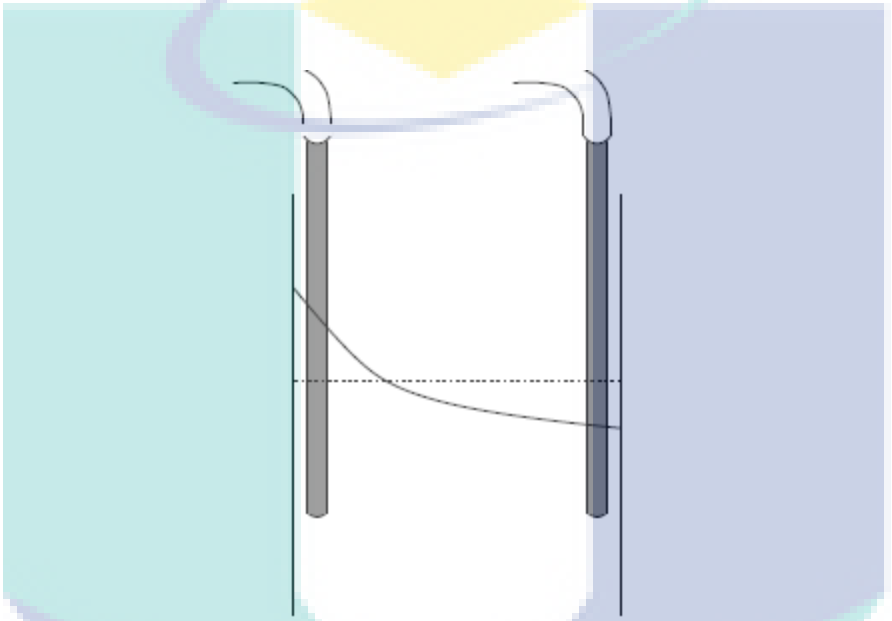

Figure 2.2: Illustration of the pressure sensor

2.2.3 Ultrasonic Measurement

When it comes to measure the level of slosh of course is involve the level of the liquid. An ultrasonic sensor has been considered to use in this project to detect the slosh. By locating the sensor on the top of the container this sensor be able to give a result of the liquid level as shown in Figure 2.3. As the result, the sensor gives a promising reading value when the surface of the liquid at rest condition and when there is small movement of the surface liquid. But, when the surface was moving to wildly, the sensor produce erroneous level reading [12]. Due to this erroneous reading, ultrasonic sensor is not suitable use to measure the height of the wave.

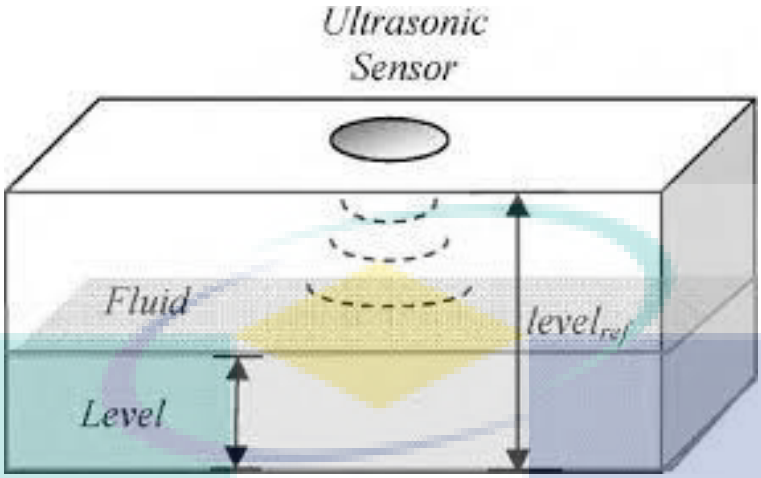

Figure 2.3: Illustration of the ultrasonic sensor

The ultrasonic sensor is not suitable in this project because during the small slosh the sensor will have many error readings due to the surface of the liquid that is not in steady mode. The signal that transmits from the transmitter will propagate too many directions due to the liquid surface. It can be clearly seen in Figure 2.4. Because of the surface of the liquid is unstable the receiver will not receive the signal that has been transmit and few reading data will loss.

Figure 2.4: Propagation of signal

2.2.4 Optical Measurement

Many sensors have been tried to measure the liquid slosh and most of it is the contact type sensor detection. The basic principle of this technique is to get the data of the wave image by using camera. Another optical measurement, such as laser Doppler velocimetry is based on Doppler Effect [13]. The light wave changes due to the condition of the wave, which is the way of this method to measure elevation of the liquid surface. The main idea of this technology is to shoot a laser sheet onto the experimental wave and produce a light line on the surface. This is shown in Figure 2.5.

This method can be used to detect slosh but there is some problem need to be considered to get accurate result. The problem is to deal with the detect range on liquid surface [13]. This technology has is unique and has its own advantage, because of the laser beam unexpanded the light illumination area on liquid surface is small. The sloshing wave is considered as plane wave only in the case of the small illumination area. Because of this problem, there will be minimum range of the measurement and the sloshing wave become more complex.

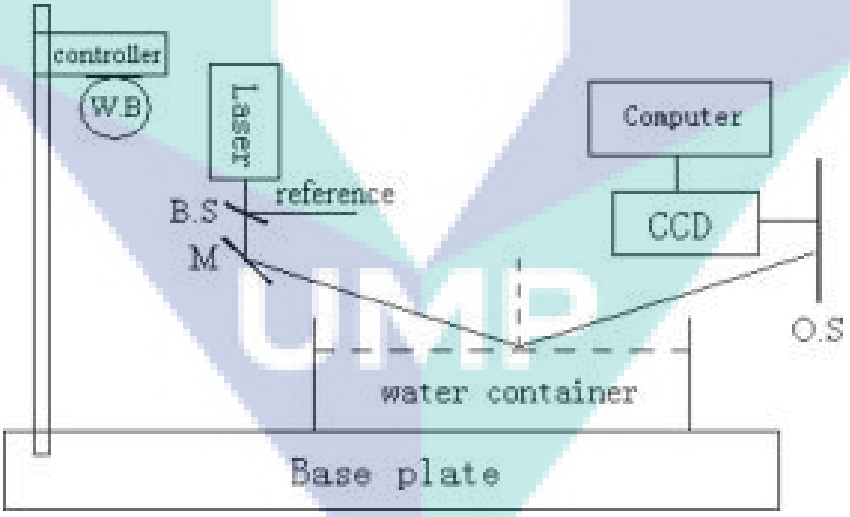

Figure 2.5: Illustration of optical measurement

2.2.5 Electrical Contact Based Measurement

In this method, the water is use as electrical conductivity to measure the liquid surface. The sensor is made up 14 pin that are attach to the wall of the container and one ground plate. Each of the pin is separated by 5mm away from each other. The experiment setup is

shown as in Figure 2.6. The cause of this method not preferred to us is due to the low accuracy during the small slosh experiment. There were also some minor problems with water drops attached to the pins and the thin layer of water formed on the package wall [14].

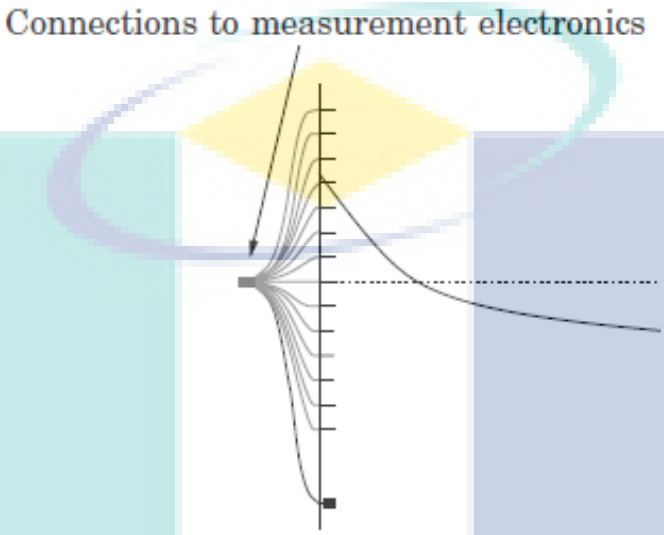

Figure 2.6: Experiment setup on electrical measurement

2.3 Nonlinear Identification for Liquid Slosh Modeling

Nowadays, liquid slosh inside a cargo always happens in many situations. For example, ships with liquid container carriers are at high risk of generating sloshing load during operation. In the metal industries, high oscillation can spill molten metal that is dangerous to the operator. Meanwhile, sloshing of fuel and other liquids in moving vehicles may cause instability and undesired dynamics. Hence, it is necessary to completely study the behavior of this residual slosh induced by the container motion. One may study the behavior of liquid slosh through developing the exact mathematical model of liquid slosh. So far, many researchers focus on the first principle approach to model the slosh behavior, while there are few literatures to discuss it from the perspective of nonlinear system identification approach.

On the other hand, block oriented nonlinear system identification has become a popular technique to model a complex plant. The block oriented nonlinear model can be classified into three categories, which are Hammerstein model, Wiener model and Hammerstein Wiener model. In particular, Hammerstein model is a model that consists of a nonlinear function followed by linear dynamic sub-plant, while Wiener model consists of a linear

dynamic sub-plant followed by nonlinear function, and finally, Hammerstein-Wiener model contains a linear dynamic sub-plant inserted between two or more nonlinear functions in series. Among these three block-oriented models, Hammerstein model is famous due to its simple model structure and it has been widely used for nonlinear system identification. Specifically, the Hammerstein model has been applied to model a real plant such as Solid Oxide fuel cell [15], bidirectional DC motor [16], oxygen uptake estimation [17], stretch reflex dynamics [18], turntable servo system [19], pneumatic muscle actuators [20], amplified piezoelectric actuators [21] and multi-axis piezoelectric micro positioning stages [22]. On the other hand, there are many tools that have been utilized to identify the Hammerstein model. There are the iterative method [23]-[25], the subspace method [26]-[28], the least square method [29], the blind approach [30] and the parametric instrumental variables method [31]. Moreover, many also consider the optimization tools for Hammerstein model, such as Bacterial Foraging algorithm [32], Cuckoo search algorithm [33], Particle Swarm optimization [34], and Genetic algorithm [35].

Based on the above literature, several limitations are ineluctable in their works, which are:

(i) Most of the Hammerstein models used in their study are based on discrete-time model, while many real plants can be easily represented in continuous-time model.

(ii) Almost all the methods assume a known structure of nonlinear function, which consists of several basis functions.

Though, our proposed work can solve a more general class of continuous-time Hammerstein model by assuming an unknown structure of nonlinear function. In particular, a piece-wise affine function is adopted with so many basis functions. Due to the introduction of the piece-wise affine function, a high dimensional design parameter tuning is considered in this study, which make the identification problem more complex.

Chapter 3

Liquid Slosh Sensor and Modelling

3.1 Liquid Slosh Sensor Development

3.1.1 Overview of Liquid Slosh Sensor Design

This project is involving communication between hardware and software. For the hardware, the accelerometer is connected with Arduino Uno, while for the software, the LabVIEW platform is used. Figure 3.1 shows the block diagram of the communication between LabVIEW, Arduino UNO, sensor and liquid slosh plant. In particular, the platform is designed such that it can monitor the behaviour of the slosh using the accelerometer as the sensor. Here, the Arduino Uno acts as controller of the system to control or manage the data between sensor and LabVIEW. There is communication between the Arduino and the LabVIEW for displaying graph of the sensor. Besides that, Arduino UNO also gives the voltage input to the remote-control car so that the remote-control cars have a constant voltage supply. The LabVIEW will display graph of the sensor in real-time. The system will start after the Arduino UNO supply the voltage to the remote-control car, meanwhile the sensor also simultaneously active when the surface of the water produces slosh or movement.

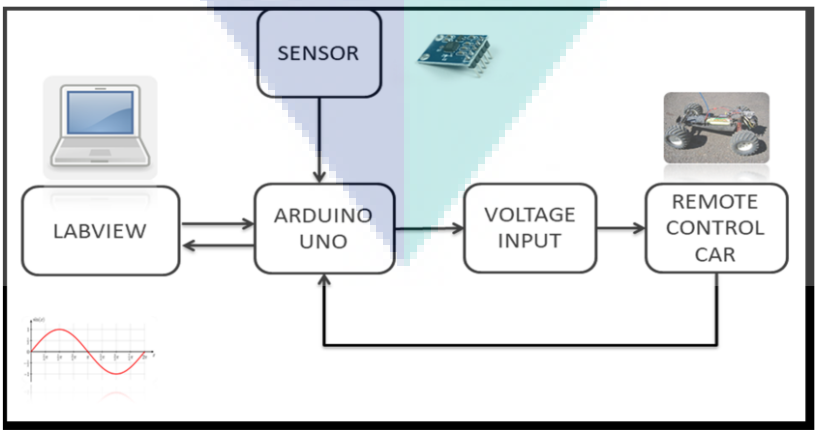

Figure 3.1: Block diagram communication of the system

The circuit diagram of the system is shown in Figure 3.2. In the circuit diagram the sensor is connected to the 5 volt of input voltage from the Arduino. This is because; 3.3 volt of voltage supply to the sensor is suitable when using one sensor only. In this project 3 sensors are used to monitor the behaviour of the slosh. Thence, 5 volts is used to ensure that the voltage supply for the sensor is sufficient for the sensor to operate successfully. It has been noticed that only z-axis is used for each sensor. Therefore, it is enough to use Arduino UNO for this project.

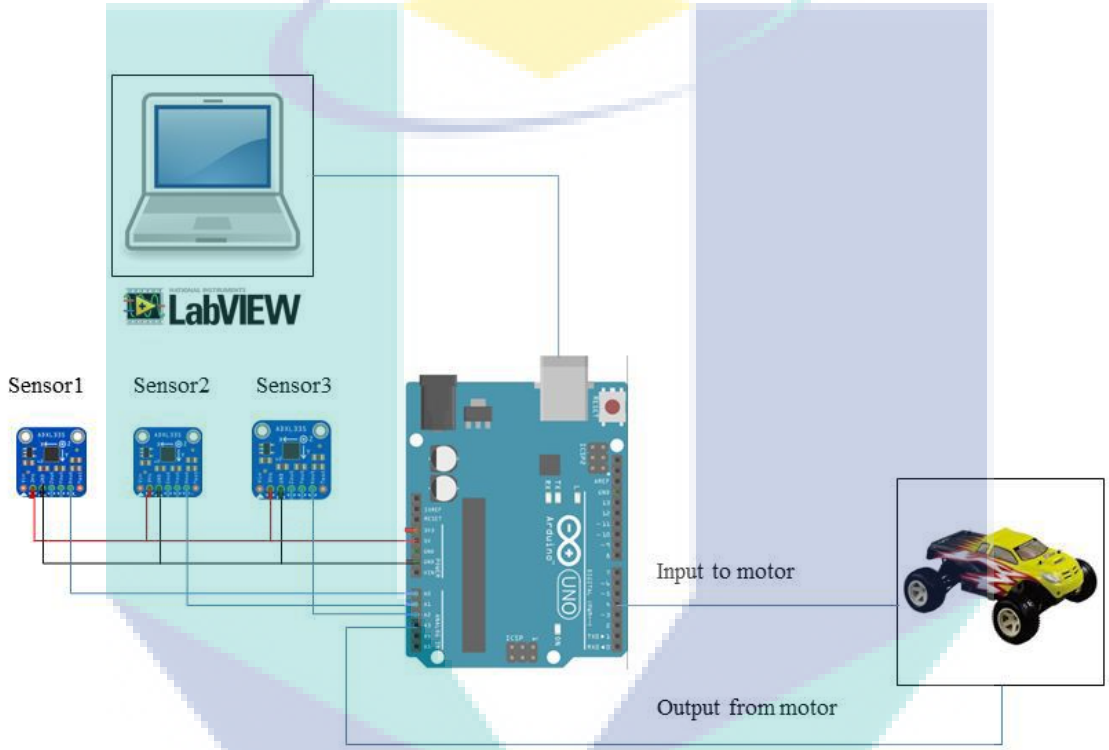

Figure 3.2: Circuit diagram of the system

3.1.2 Components and Tools for Liquid Slosh System

A. Arduino UNO

The main equipment use in this project is Arduino UNO. Arduino UNO is act as the controller in this system. Arduino Uno is a microcontroller board based on the Microchip ATmega328P microcontroller and made by Arduino. The board contain digital and analog pin. It can be set as the input or output that can be interface with other circuit. There are 14 digital pins, 6 analog pins, output source pins 5 volt and 3.3 volt, and it can communicate with the computer with programmable Arduino IDE (Integrated

Development Environment) using type B USB cable. The Arduino can be powered using 9 volts battery and the range power can be supply to the Arduino is between 7 to 20 volts. The analog and digital pin can provide and receive 5 volts for each pin. Also, it can receive 20 mA of current in its operating condition. Besides that, in this project to communicate with Arduino, we must upload coding of certain program into the Arduino first. After that, we use the pin as input or output that has been set in the coding. To communicate with the LabVIEW software LINX wizard must be uploaded into the Arduino.

B. Accelerometer ADXL335 with 3 Axes

Figure 3.3 shows the ADXL334 with 3 axes. This ADXL335 sensor has three-axis which contains analogue accelerometer IC. This sensor read from x, y and z axes acceleration according to the gravity. An accelerometer an accelerometer can sense the movement or the direction of the moving device and how fast the device is moving. The current required for the sensor typically falls in milliamp or the micro(μ) range, where the ADXL335 is a triple axis (x. y, z) accelerometers with low power consumption and low noise at 320μA. The on-board voltage regulations, which enable from 3V to 6V power of the board, include the bandwidth of each axis to 50Hz and 0.1μF capacitors set.

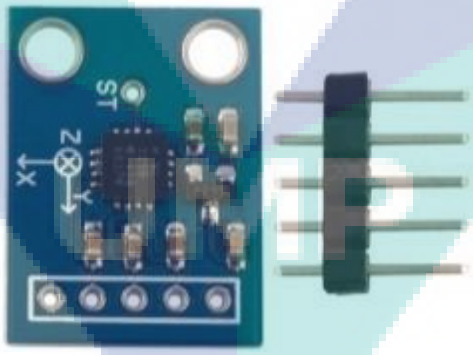

Figure 3.3: Accelerometer ADXL 335 with 3 axes

C. Floating Platform

In order to make sensor to detect the reading of the slosh using the accelerometer is that the sensor need to be on the liquid. Therefore, the idea is to make a device that is floating on the liquid and the design should be waterproof so that it can protect the sensor from wet. This kind of design actually inspired by the structure of fish cupula, especially when

several sensors are put on the floating platform. The dimension of the floating device is 18.5cm x 2.5cm x 2.5cm (length x width x height). The position of the sensors on the floating platform is shown in Figure 3.4. The side of the floating device is cover with the white form. This is because to keep the device floating on the surface of the water. In order to make the device float, polystyrene has been applied around the device so that is will float on the liquid.

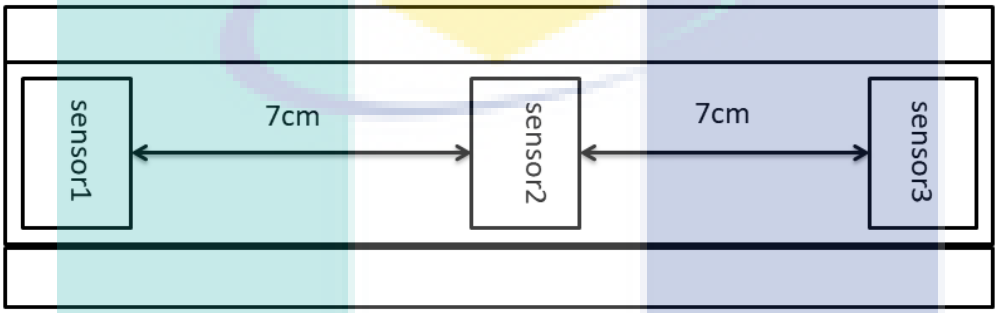

Figure 3.4: Position of sensor on floating device

It also consists of minimum full-scale range of ±3 g product acceleration measurement and dynamic acceleration resulting from vibration, motion and shock. Furthermore, it also can measure the static movement or static acceleration due of gravity in tilt sensing application. The XOUT, YOUT, and ZOUT capacitor at the CX, CY, and CZ pin, respectively, can be selected to adjust the bandwidth of the accelerometer by user. The bandwidth range is selected such that it suits with the application. In particular, the range from 0.5 Hz to 16000 Hz for the x and y-axis and from 0.5 Hz to 550 Hz for the z-axis.

D. Remote Control Car

Remote control car is used in this project to generate the movement of the liquid tank. The idea is to pull the tank according to the several pre-determined input voltages. The variation of the input voltage applied to the remote car is required to monitor the behaviour of the liquid slosh. This remote-control car is 1.243kg weight and the size is 215.5cm x 26.5cm x 12.5cm (L x W x H). The control distance from the transmitter to the receiver of the car is in 60 cm plus the playing time for the remote-control car, which is 20-25 minutes.

Here, EcoSport Rc Car has been chosen to pull the liquid container. To make movement of the tank, the remote car must have powerful motor that available to pull tank that have

weight of 1 kilogram. Besides that, rubber tire is play important role so that the tank moves smoothly. This remote-control car operates at 12V maximum voltage of 700mAh Ni-cd battery and it applicable at grassy land, rocky land sandy land and road. With 5volt of voltage applied, it is considered to be powerful enough to pull the liquid tank which has the weight of 1 kilogram.

E. Liquid Container

The liquid container used in this project is made up from plastic. This is because, many researchers preferred to use rigid type material, less weight and simple design. The size of the container is 21cm x 12.5cm x 13cm (L x W x H) and the volume of the water use in the experiment is 2.1 liter. The volume of water used in this study is enough to create the liquid slosh and it does not spill out from the container during the experiment. The volume of the water needs to be fixed because, it will affect the reading of the slosh when the container is moved.

Figure 3.5: Liquid Container

At the bottom of the container four wheels are attached at each of the corner of the container. The use of these wheels is to reduce the friction and to make the container move more easily. At the right side of the container there is a plastic plate attach to the body of the container. The function of plastic plate is to make contact or connection between the remote-control car and liquid container. The distance between the container and the remote-control car is around 3cm as shown in Figure 3.6. The wheels that attached to the container have 2cm of diameter and 1cm of tire width. The height of the container from the floor is 3cm. Meanwhile, the height body of the remote-control car

from the floor is 6cm and the width of the car is 26.5cm.

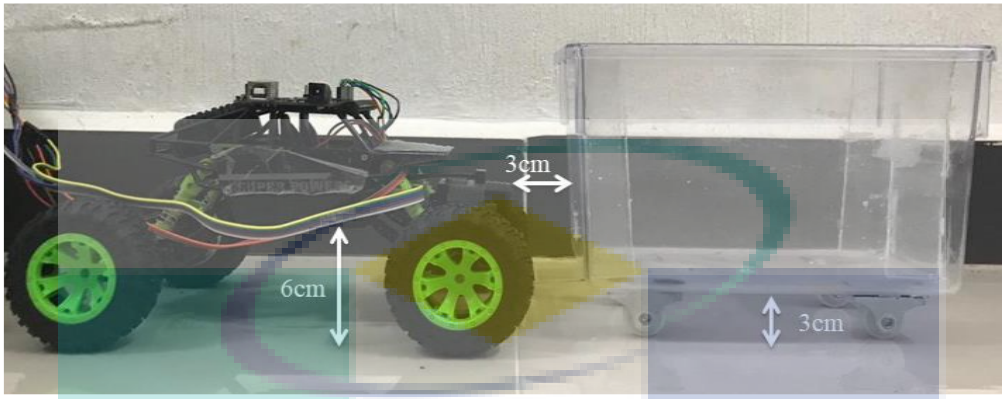

Figure 3.6: Connection between liquid container and remote-control car on side view

F. LabVIEW

LabVIEW is the platform that is used in this project to display graph and to monitor the behaviour of the liquid slosh. To enable the Arduino to communicate with the LabVIEW, firstly, the Arduino must be uploaded using the LINX Firmware Wizard. This is because, the LINX Firmware Wizard is suitable to use with Vis for interfacing with the Arduino. Hence, the communication between LabVIEW and the Arduino can be executed.

After the firmware has been uploaded, the Arduino can communicate with the LabVIEW. This is very important process on this project since it will capture the liquid slosh data and further signal conditioning can be made through the LabVIEW platform. The LabVIEW display the graph in real-time condition of the sensor data. So, USB cable must be connected from the computer to the Arduino board all the time and this USB cable is the medium of the data to be transferred from Arduino to the LabVIEW.

3.1.3 Process Flow of Sensor Verification

The process flow for the sensor to detect reading on the behaviour of the slosh is described in this section. By initializing the LabVIEW software, the LINX firmware wizard must be setup before the Arduino and the LabVIEW communicate between each other. When the Arduino connect to the laptop, it automatically switches on and ready to be used. By choosing the correct COM port, the LabVIEW will start monitoring the behaviour of the liquid slosh data from the sensor.

Meanwhile, the Arduino UNO gives the input voltage to the remote-control car to move and stop automatically according to time that has been set. Here, the input voltage graph is also recorded in real-time and in time domain with amplitude of voltage value. This is because, Analog Read 1 can read the value of the specified analog input channel and returns the analog value in volts.

3.2 Modelling of Liquid Slosh using Nonlinear System Identification

In this section, the proposed Sine Cosine Algorithm (SCA) for identification of liquid slosh plant in Subchapter 3.1 based on Hammerstein model is presented. Firstly, a problem formulation to identify the liquid slosh plant is explained. Then, it is shown on how to apply the SCA method to identify the liquid slosh based on Hammerstein model. Figure 3.7 shows a complete block diagram to identify the liquid slosh model in Subchapter 3.1. The proposed Hammerstein model consists of nonlinear function $h(u)$ followed by the transfer function $G(s)$. The nonlinear function is a piece-wise affine function given by

$$h(u)=\begin{cases} c_0+m_1(u-d_0) & \text{if} \quad d_0 \le u < d_1, \\ c_1+m_2(u-d_1) & \text{if} \quad d_1 \le u < d_2, \\ \vdots & \\ c_{\sigma-1}+m_\sigma(u-d_{\sigma-1}) & \text{if} \quad d_{\sigma-1} \le u < d_\sigma, \end{cases} \tag{3.1}$$

and the transfer function $G(s)$ is given by

$$G(s)=\frac{B(s)}{A(s)}=\frac{s^m+b_{m-1}s^{m-1}+\cdots+b_0}{a_m s^m+a_{m-1}s^{m-1}+\cdots+a_0}. \tag{3.2}$$

In (3.1), the symbol $m_i=(c_i-c_{i-1})/(d_i-d_{i-1})\,(i=1,2,...,\sigma)$ are the segment slope with connecting input and output points as $d_i\,(i=0,1,...,\sigma)$ and $c_i\,(i=0,1,...,\sigma)$, respectively. For simplicity of notation, let $\boldsymbol{d}=[d_0, d_1, \ldots, d_\sigma]^{\mathrm{T}}$ and $\boldsymbol{c}=[c_0, c_1, \ldots, c_\sigma]^{\mathrm{T}}$. Note that the total number of input or output points are $\sigma+1$. The input of the real liquid slosh plant and the identified model is defined by $u(t)$, while the output of the real liquid slosh plant and the identified model are denoted by $y(t)$ and $\tilde{y}(t)$, respectively. Thence, the expression of the identified output can be written as

$$\tilde{y}(t)=G(s)h(u(t)). \tag{3.3}$$

Moreover, several assumptions are adopted in this work, which are:

(i) The order of the polynomial $A(s)$ and $B(s)$ are assumed to be known

(ii) The nonlinear function $h(u(t))$ is one-to-one map to the input $u(t)$ and the values of $d_i\,(i=1,2,...,\sigma)$ are pre-determined according to the response of input $u(t)$.

Next, let t_s be a sampling time for the real experimental input and output data ($u(t)$, $y(t)$) ($t = 0, t_s, 2t_s, \ldots, Nt_s$). Then, in order to accurately identify the liquid slosh model, the following objective function in (3.4) is adopted in this study:

$$E(G,h) = \sum_{\eta=0}^{N} \left(y(\eta t_s) - \tilde{y}(\eta t_s)\right)^2 . \tag{3.4}$$

Note that the objective function in (3.4) is based on the sum of quadratic error, which has been widely used in many literatures. Finally, our problem formulation can be described as follows.

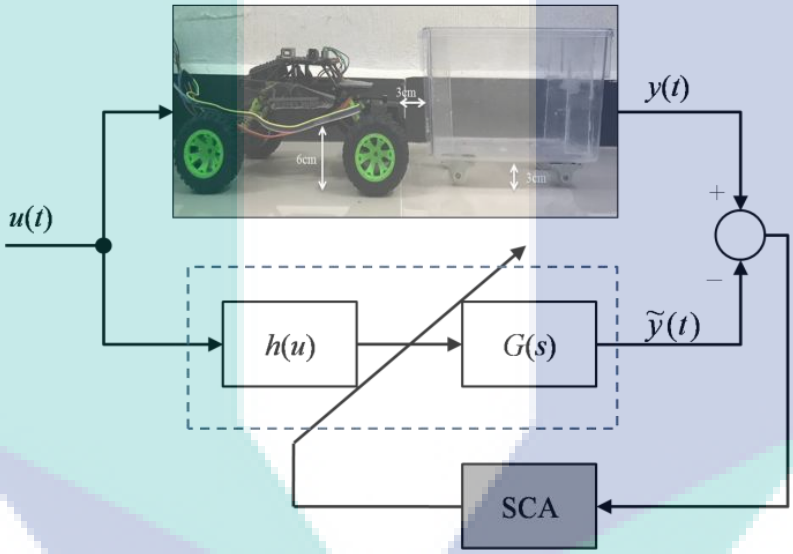

Figure 3.7: Block diagram of Hammerstein model based SCA

Problem 1. Based on the given real experimental data ($u(t)$, $y(t)$) in Figure 3.7, find the nonlinear function $h(u)$ and the transfer function $G(s)$ such that the objective function in (3.4) is minimized.

Furthermore, it is shown on how to apply the SCA in solving **Problem 1**. For simplicity, let the design parameter of **Problem 1** is defined as $\boldsymbol{x} = [b_0 \quad b_1 \quad \cdots \quad b_{m-1} \quad a_0 \quad a_1 \quad \cdots \quad a_m \quad c_0 \quad \cdots \quad c_\sigma]^{\mathrm{T}}$, where the elements of the design parameter are the coefficients of both the nonlinear function and the transfer function of the continuous-time Hammerstein model. In SCA framework, let $\boldsymbol{x}_i \, (i = 1,2,\ldots,M)$ be the design parameter of each agent i for M total number of agents.

Then, consider $x_{ij}(j=1,2,...,D)$ be the j-th element of the vector $\boldsymbol{x}_i(i=1,2,...,M)$, where D is the size of the design parameter. Thence, by adopting objective function in (3.4), a minimization problem is expressed as

$$arg \min_{\boldsymbol{x}_i(1),\, \boldsymbol{x}_i(2),...} E(\boldsymbol{x}_i(k)). \tag{3.5}$$

for iterations $k = 1, 2, \ldots$, until maximum iteration k_{max}. Finally, the procedure of the SCA in solving **Problem 1** is shown as follows:

Step 1: Determine the total number of agents M and the maximum iteration k_{max}. Set $k = 0$ and initialize the design parameter $\boldsymbol{x}_i(0)(i=1,2,...,M)$ according to the upper bound $\boldsymbol{x}_{up}$ and lower bound $\boldsymbol{x}_{low}$ values of the design parameter.

Step 2: Calculate the objective function in (3.4) for each search agent i.

Step 3: Update the values of the best design parameter $\boldsymbol{P}$ based on the generated objective function in **Step 2**.

Step 4: For each agent, update the design parameter using the following equation:

$$x_{ij}(k+1) = \begin{cases} x_{ij}(k) + r_1 \sin(r_2) \times \left\| r_3 P_j - x_{ij}(k) \right\| & \text{if} \quad r_4 < 0.5, \\ x_{ij}(k) + r_1 \cos(r_2) \times \left\| r_3 P_j - x_{ij}(k) \right\| & \text{if} \quad r_4 \geq 0.5, \end{cases} \tag{3.6}$$

where

$$r_1 = 2\left(1 - \frac{k}{k_{\max}}\right) \tag{3.7}$$

for maximum iteration k_{max}. Note that r_2, r_3 and r_4 are random values that are generated independently and uniformly in the ranges $[0, 2\pi]$, $[0, 2]$ and $[0, 1]$, respectively. The detailed justification on the selection of the coefficients r_1, r_2, r_3 and r_4 are clearly explained in [36]. In (3.6), the symbol $P_j (j = 1, 2, ..., n)$ is denoted as the best current design parameter in j-th element of $\boldsymbol{P}$ that is kept during tuning process.

Step 5: After the maximum iteration is achieved, record the best design parameter $\boldsymbol{P}$ and obtained the continuous-time Hammerstein model in Figure 3.7. Otherwise, repeat **Step 2**.

Chapter 4

Results and Discussions

This chapter is divided into two parts, which are the results and analysis of the liquid slosh data based on the designed sensor and the analysis of the developed liquid slosh model based on nonlinear Hammerstein system. The first part involves the analysis of the suitable volume of liquid for better sensor reading and the analysis of suitable input voltage to produce acceptable liquid oscillation. Meanwhile, the latter part focuses on the analysis of the developed model in nonlinear function and linear system, in terms of time domain and frequency domain analysis.

4.1 Analysis of the Data from Liquid Slosh Sensor

4.1.1 Analysis of the Sensor Reading with Respect to Volume of Water

The volume of the water plays important role in this experiment. This is because, the mass of the water depends on the volume and the density of water as the formula mass state mass = volume x density. As for the water density, it has been fixed that the density of water is 997kg/m3. This also give an impact to the voltage input because when the container is lighter the less voltage is used to move the container. Also, it is easier to create the slosh using low voltage. Even that so, there is disadvantageous when the amount of liquid is small. An experiment is conducted to see the suitable volume of liquid to fill in the container.

Table 4.1 shows the suitable condition of the sensor that is depending on the water volume and the input voltage. As shown in the table, the lower volume of the water is not suitable for the investigation. This is because, the floating device will make contact with the bottom of the container and produce unfeasible sensor reading. For 1.5 liter of water, it is almost suitable to be used in the investigation and the water height just above half of the container can be used but not too accurate. The suitable volume is 2.0 liter of water.

This is because, the water is fill ¾ of the container and most of the researchers commonly used this setting in their investigations. Moreover, this level is suitable because, all input voltage that is used in the experiment is acceptable by using this volume of water.

Table 4.1: Effect of voltage input to the Volume of water and condition of sensor

Input Voltage (V)	Water Volume (L)	Sensor Reading	
1.5	0.5		Bad
	1.0	Good	
	1.5	Good	
	2.0	Good	
3	0.5		Bad
	1.0		Bad
	1.5	Good	
	2.0	Good	
5	0.5		Bad
	1.0		Bad
	1.5	Good	
	2.0	Good	
7	0.5		Bad
	1.0		Bad
	1.5		Bad
	2.0	Good	
10	0.5		Bad
	1.0		Bad
	1.5		Bad
	2.0	Good	

4.1.2 Analysis of the Sensor Reading with Respect to the Input Voltage

Voltage input is the voltage applied to the remote-car and consequently move the container. As a result, a liquid slosh oscillation is produced. Early hypothesis that can be stated is the higher the voltage input value, the higher the slosh produced. This hypothesis can be proven by real-time simulation using LabVIEW as an analysis platform to observe the conditional wave generated.

The experiment is about measuring slosh with suitable or optimum input voltage applied to the remote-control car. When the input voltage is applied to the car for 4s, the sensor also shows reading same duration as the input voltage. This proves that the reading of the sensor is correlated with the reading of the voltage input. Besides that, in the experiment, we also need to find the optimum amplitude of input voltage applied to the car for making the slosh reading more accurate.

Table 4.2 shows the reading of the sensor from several input voltage that is applied to the remote-control car. The reading also represents the maximum amplitude or height of the slosh when the container of the liquid moving. From the table, it can be concluded that the higher the input voltage, the higher the peak reading of the sensor. The suitable input voltage that can be applied to the remote-control car is 5V. This is because; the input voltage of 5V is already giving good reading of the sensor as also been clarified in Table 4.1. Furthermore, the size of the container is small while too much force acting on the container will spill out the liquid from the container.

Table 4.2: Relations between the input voltage and the maximum amplitude of the slosh

Input Voltage (V)	Sensor 1 (cm)	Sensor 2 (cm)	Sensor 3 (cm)
1.5	0.60	0.65	0.65
3	0.70	0.75	0.75
5	0.90	0.75	0.90
7	1.00	0.90	1.00
10	1.25	1.10	1.20

Based on the analysis in Tables 4.1 and 4.2, the generated input voltage in Figure 4.1 is used as the suitable input applied to remote car to produce good liquid slosh reading. Figure 4.2 shows the response of the liquid slosh from one of the sensors. The response or the output data in Figure 4.2 will be used to identify the dynamic model of the liquid slosh.

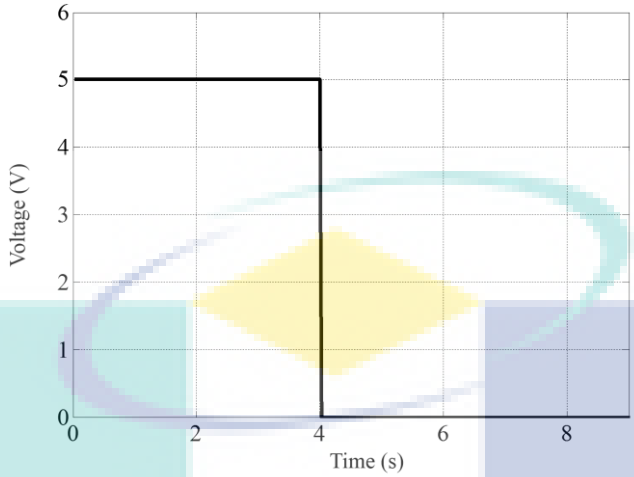

Figure 4.1: Input voltage applied to the remote car

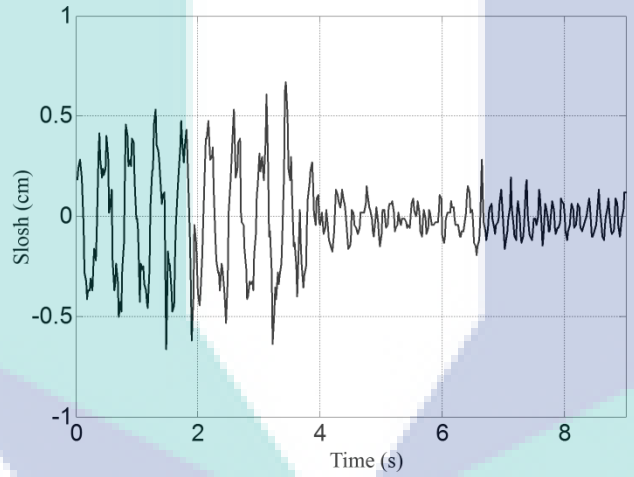

Figure 4.2: Output slosh from the accelerometer sensor

4.2 Results and Analysis of Liquid Slosh Model

In this section, the effectiveness of the SCA based method for identifying the liquid slosh system using continuous-time Hammerstein model is demonstrated. In particular, the convergence curve response of the objective function in (3.4), the pole-zero mapping of linear function and the plot of nonlinear function, will be presented and analyzed in this study.

Based on the experimental setup in Chapter 3, the input response $u(t)$ as shown in Figure 4.1 is applied to the liquid slosh plant, and the output response $y(t)$ is recorded as shown in

Figure 4.2. Here, the input and output data are sampled at t_s = 0.02 s for N = 450. In this study, the structure of $G(s)$ is selected as follows:

$$G(s) = \frac{B(s)}{A(s)} = \frac{s^3 + b_2 s^2 + b_1 s + b_0}{a_4 s^4 + a_3 s^3 + a_2 s^2 + a_1 s + a_0}. \quad (4.1)$$

after performing several preliminary testing on the given data ($u(t)$, $y(t)$). The fourth order system is used by considering a cascade of 2nd order system for both dc motor of remote car and the slosh dynamic. Meanwhile, the input points for piece-wise affine function of $h(u(t))$ are given by $\boldsymbol{d}$ = [0, 0.2, 0.4, 0.6, 0.8, 1, 2, 3, 4, 5]^T. The selection of vector $\boldsymbol{d}$ is obtained after several preliminary experiments. The design parameter $\boldsymbol{x} \in \boldsymbol{R}^{18}$ with its corresponding transfer function and nonlinear function is shown in Table 4.3. Next, the SCA algorithm is applied to tune the design parameter with initial values of design parameter are randomly selected between the upper bound $\boldsymbol{x}_{\text{up}}$ and lower bound $\boldsymbol{x}_{\text{low}}$ as shown in Table 4.3. Note that the values $\boldsymbol{x}_{\text{up}}$ and $\boldsymbol{x}_{\text{low}}$ are obtained after performing several preliminary experiments. Here, we choose the number of agents M = 40 with maximum iterations $k_{\max}$ = 5000.

Table 4.3: Design parameter of liquid slosh plant

$\boldsymbol{x}$	Coefficients	$\boldsymbol{x}_{\text{low}}$	$\boldsymbol{x}_{\text{up}}$	$\boldsymbol{P}$
x_1	b_2	–5	35	–3.7948
x_2	b_1	–5	35	10.7153
x_3	b_0	–5	35	–0.9059
x_4	a_4	–5	35	–0.6154
x_5	a_3	–2200	–1	–5.3112
x_5	a_2	–2200	–1	–139.8711
x_7	a_1	–2200	–1	–1132.2883
x_8	a_0	–2200	–1	–839.7621
x_9	c_0	–5	5	–4.8859
x_{10}	c_1	–5	5	–0.0219
x_{11}	c_2	–5	5	3.3211
x_{12}	c_3	–5	5	–4.7295
x_{13}	c_4	–5	5	–0.3240
x_{14}	c_5	–5	5	–4.4858
x_{15}	c_6	–5	5	-0.0002
x_{16}	c_7	–5	5	0.0000
x_{17}	c_8	–5	5	0.1679
x_{18}	c_9	–5	5	–4.3282

Figure 4.3 shows the response of the objective function convergence with the value of $E(G,h)$ = 0.1616 at k_{max} = 5000 with 80.44 % of objective function improvement to produce the best design parameter ***P*** as shown in the final column of Table 4.3. It shows that the SCA based method is able to minimize the objective function in (3.4) and produce a quite close output response $y(t)$ as compared to the real output $\tilde{y}(t)$, which can be clearly seen in Figure 4.4. Note that the identified output response tends to yield high oscillation when input is injected to the system and it start to attenuate when the input is zero, which is quite similar to the response of real experimental output.

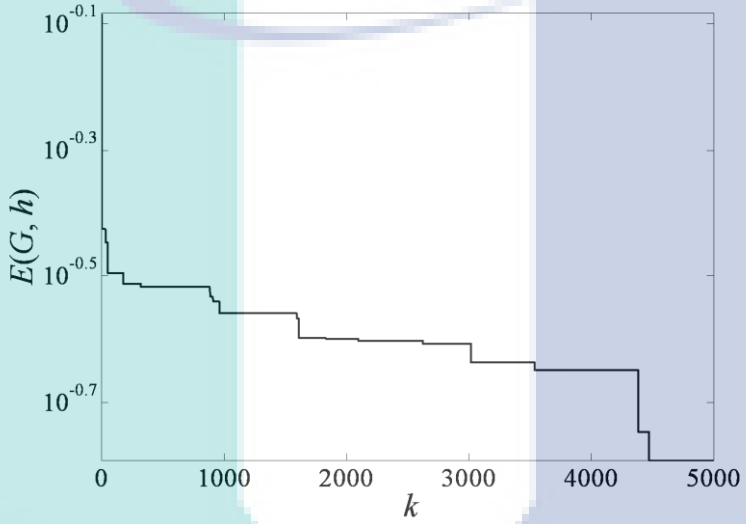

Figure 4.3: Convergence curve response

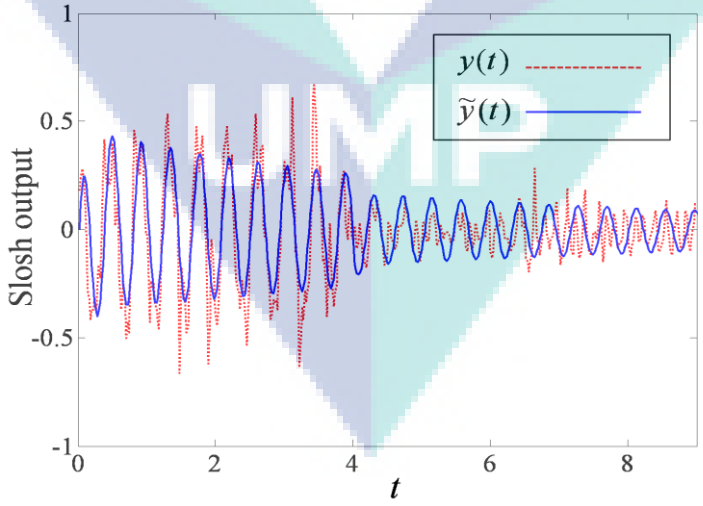

Figure 4.4: Response of the identified output $\tilde{y}(t)$ and real output $y(t)$

In the real experimental setup, we can say that the liquid slosh system is stable since the liquid slosh output is reduced gradually as $t \to \infty$. In order to validate our model regarding the stability, we use the pole-zero map of the identified transfer function $G(s)$ as shown in Figure 4.5. From the pole-zero map, all the poles are located at the left-hand side of y-axis. In particular, the obtained values of poles are $-0.1190 \pm j14.8001$, -7.5621 and -0.8229, while the obtained values of zeros are 0.0872 and $1.8538 \pm j2.6373$. On the other hand, we also can observe the feature of nonlinear function by plotting the obtained piece-wise function as depicted in Figure 4.6. Note that our nonlinear function is not restricted to any form of nonlinear function (i.e., quadratic), which is more generalized and provide more flexibility of searching a justifiable function.

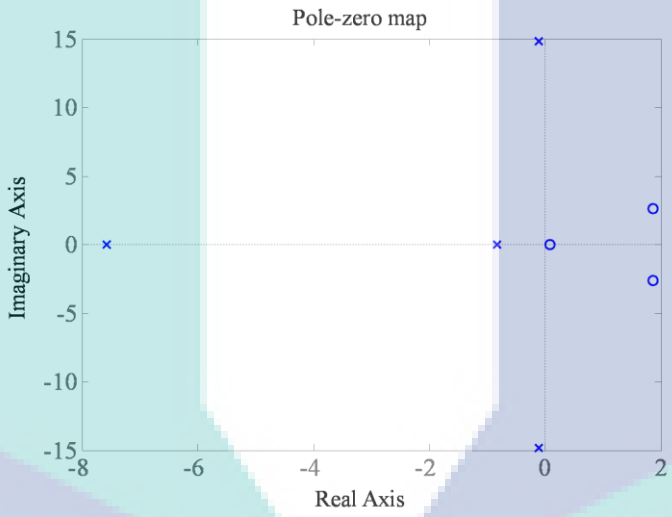

Figure 4.5: Pole-zero map of transfer function $G(s)$

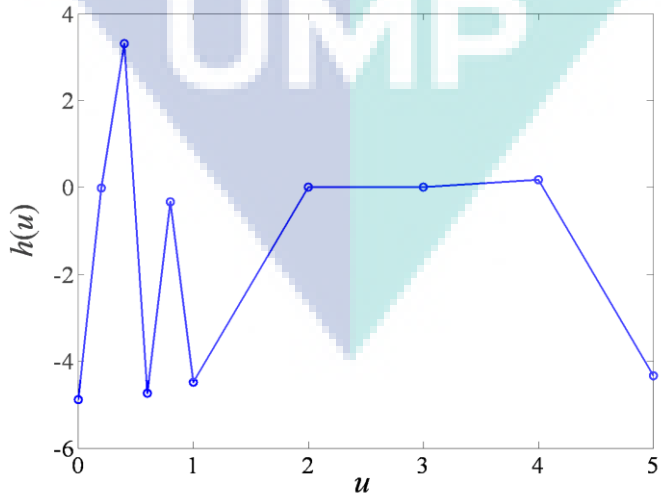

Figure 4.6: Resultant of piece-wise affine function $h(u)$

Chapter 5

Conclusion

As the conclusion, the accelerometer sensors that measure the liquid slosh behavior have been developed. Here, only the Z axis motion of slosh is considered, while the X axis and Y axis is not affected the reading of the slosh because of the slosh only moves vertically. Three slosh sensors which are in series and replicate the fish cupula behavior are used to record the slosh data simultaneously. Moreover, LINX is the key to make the LabVIEW and the Arduino to communicate with the proposed sensors. Besides that, several investigations are conducted to observe the feasibility of the proposed sensor. Firstly, the analysis of the amount of water with respect to sensor reading is shown. Secondly, the analysis of size of input voltage with respect to sensor reading is presented. Based on both analyses, it is shown that the input voltage of 5 volts that is run for 4 s and ¾ of liquid in the container are selected as the optimum setting to generate an accurate slosh sensor reading.

In this project, an identification of liquid slosh behaviour using continuous-time Hammerstein model based on Sine Cosine Algorithm (SCA) has also been presented. The results demonstrated that the proposed generic Hammerstein model based on SCA has a good potential in identifying the real liquid slosh behavior. In particular, it is shown that the proposed method is able to produce a quite close identified output with real liquid slosh output. Moreover, the resultant linear model has been proved to be stable based on the pole-zero map. It is also shown that the used of piecewise-affine function gives more flexibility for the SCA to search more generic nonlinear function. In the future, our work can be extended to various types of nonlinear function such as continuous-time Wiener and Hammerstein-Wiener.

References

1. E. Rizzuto and R. Tedeschi, “Surveys of actual sloshing loads on board of ships at sea”, in *proceedings of International Conference on Ship and Marine Research*, pp. 7.29-7.37, 1997.
2. K. Terashima and G. Schmidt, “Sloshing analysis and suppression control of tilting-type automatic pouring machine”, in *proceedings of IEEE International Symposium on Industrial Electronics*, pp. 275-280, 1994.
3. T. Acarman and U. Ozguner, “Rollover prevention for heavy trucks using frequency shaped sliding mode control”, *Vehicle System Dynamics*, Vol. 44(10), pp. 737-762, 2006.
4. A. Aboel-Hassan, M. Arafa and A. Nassef, “Design and optimization of input shapers for liquid slosh suppression”, *Journal of Sound and Vibration*, Vol. 320(1-2), pp. 1-15, 2009.
5. M. Grundelius, Methods for control of liquid slosh. PhD thesis, Lund Institute of Technology, 2001.
6. B. Pridgen, K. Bai and W. Singhose, “Slosh suppression by robust input shaping”, in *proceedings of IEEE Conference on Decision and Control*, pp. 2316-2321, 2010.
7. B. Pridgen, K. Bai and W. Singhose, “Shaping Container Motion for Multimode and Robust Slosh Suppression”, *Journal of Spacecraft and Rockets*, Vol. 50(2), pp. 440-448, 2013.
8. M.N.M. Nawi, A.A. Manaf, M.R. Arshad, O. Sidek, “Fluidic based multidirectional flow sensor inspired from artificial cupula”, in *Proceedings of the 8th International Conference on Bioinspired Information and Communications Technologies*, pp. 195-198, 2014.
9. M.N.M. Nawi, A.A. Manaf, M.R. Arshad, O. Sidek, “Development of microfluidic based multidirectional flow sensor inspired from artificial cupula”, *Microsystem Technologies*, pp. 1-9, 2014.
10. E. Terzic, R. Nagarajah, M. Alamgir, “A neural network approach to fluid quantity measurement in dynamic environments”, *Mechatronics*, *21*(1), pp.145-155, 2011.
11. Z.H. Cai, D.Y. Wang, Z. Li, Z., “Influence of excitation frequency on slosh-induced impact pressures of liquefied natural gas tanks”, *Journal of Shanghai Jiaotong University (Science)*, *16*(1), pp.124-128, 2011.
12. J. Terzic, C.R. Nagarajah, M. Alamgir, “Fluid level measurement in dynamic environments using a single ultrasonic sensor and Support Vector Machine

(SVM)", *Sensors and Actuators A: Physical*, *161*(1-2), pp.278-287, 2010.

13. C.R. Zhao, L. Ye, J.F. Ge, Y. Cheng, Y., "A side-coupled optical-fiber liquid level sensor", In *Applied Mechanics and Materials* (Vol. 128, pp. 487-490). Trans Tech Publications, 2012.
14. S. Sakib, M.M. Karim, "Design and Development of a Cheap Slosh Testing Rig as Laboratory Equipment. *Procedia Engineering*, 194, pp. 401-406, 2017.
15. C. Li, *et al.*, "Identification of the Hammerstein model of a PEMFC stack based on least squares support vector machines," *Journal of Power Sources*, vol. 175, pp. 303-316, 2008.
16. T. Kara, I. Eker, "Nonlinear modeling and identification of a DC motor for bidirectional operation with real time experiments," *Energy Conversion and Management*, vol. 45, no. 7-8, pp. 1087-1106, 2004.
17. S.W. Su, *et al.*, "Oxygen uptake estimation in humans during exercise using a Hammerstein model," *Annals of biomedical engineering*, vol. 35, no. 11, pp. 1898-1906, 2007.
18. D.T. Westwick, R.E. Kearney, "Separable least squares identification of nonlinear Hammerstein models: Application to stretch reflex dynamics," *Annals of Biomedical Engineering*, vol. 29, no. 8, pp. 707-718, 2001.
19. Q. Zhang, *et al.*, "Nonlinear modeling and predictive functional control of Hammerstein system with application to the turntable servo system," *Mechanical Systems and Signal Processing*, vol. 72, pp. 383-394, 2016.
20. Q. Ai, *et al.*, "Hammerstein model for hysteresis characteristics of pneumatic muscle actuators," *International Journal of Intelligent Robotics and Applications*, vol. 3, no. 1, pp. 33-44, 2019.
21. A. Saleem, *et al.*, "Nonlinear hammerstein model identification of amplified piezoelectric actuators (APAs): Experimental considerations," *4th International Conference on Control, Decision and Information Technologies (CoDIT)*, pp. 0633-0638, 2017.
22. H.T. Zhang, *et al.*, "Distributed Hammerstein Modeling for Cross-Coupling Effect of Multiaxis Piezoelectric Micropositioning Stages," *IEEE/ASME Transactions on Mechatronics*, vol. 23, no. 6, pp. 2794-2804, 2018.
23. E.W. Bai, D. Li, "Convergence of the iterative Hammerstein system identification algorithm," *IEEE Transactions on automatic control*, vol. 49, no. 11, pp. 1929-1940, 2004.

24. J. Hou, *et al.*, "Fixed point iteration-based subspace identification of Hammerstein state-space models," *IET Control Theory & Applications*, vol. 13, no. 8, pp. 1173-1181, 2019.
25. Z. Ge, *et al.*, "Gradient-based iterative identification method for multivariate equation-error autoregressive moving average systems using the decomposition technique," *Journal of the Franklin Institute*, vol. 356, no. 3, pp. 1658-1676, 2019.
26. J. Hou, *et al.*, "Subspace Hammerstein model identification under periodic disturbance," *IFAC-PapersOnLine*, vol. 51, no. 15, pp. 335-340, 2018.
27. J. Hou, *et al.*, "Subspace identification of Hammerstein-type nonlinear systems subject to unknown periodic disturbance," *International Journal of Control*, (just-accepted), pp. 1-29, 2019.
28. I.W. Jamaludin, N.A. Wahab, "Recursive Subspace Identification Algorithm using the Propagator Based Method," *Indonesian Journal of Electrical Engineering and Computer Science*, vol. 6, no. 1, pp. 172-179, 2017.
29. D. Wang, W. Zhang, "Improved least squares identification algorithm for multivariable Hammerstein systems," *Journal of the Franklin Institute*, vol. 352, no. 11, pp. 5292-5307, 2015.
30. E.W. Bai, "A blind approach to the Hammerstein–Wiener model identification," *Automatica*, vol. 38, no. 6, pp. 967-979, 2002.
31. L. Ma, X. Liu, "A nonlinear recursive instrumental variables identification method of Hammerstein ARMAX system," *Nonlinear Dynamics*, vol. 79, no. 2, pp. 1601-1613, 2015.
32. W. Lin, P.X. Liu, "Hammerstein model identification based on bacterial foraging," *Electronics Letters*, vol. 42, no. 23, pp. 1332-1333, 2006.
33. A. Gotmare, *et al.*, "Nonlinear system identification using a cuckoo search optimized adaptive Hammerstein model," *Expert systems with applications*, vol. 42, no. 5, pp. 2538-2546, 2015.
34. H.N. Al-Duwaish, "Identification of Hammerstein models with known nonlinearity structure using particle swarm optimization," *Arabian Journal for Science and Engineering*, vol. 36, no. 7, pp. 1269-1276, 2011.
35. H. Zhang, H. Zhang, "Identification of Hammerstein Model Based on Quantum Genetic Algorithm", *Telkomnika*, vol. 11, no. 12, pp. 7206-7212, 2013.
36. S. Mirjalili, *et al.*, "Grey wolf optimizer," *Advances in engineering software*, *69*, pp. 46-61, 2014.

APPENDIX A - PUBLICATIONS

Bulletin of Electrical Engineering and Informatics
Vol. 8, No. 4, December2019, pp. ab~cd
ISSN: 2302-9285, DOI: 10.11591/eei.v8i4.xxxx

A Grey Wolf Optimizer for Identification of Liquid Slosh Behavior using Continuous-Time Hammerstein Model

Mohd Ashraf Ahmad[1], Zulkifli Musa[1], Mohd Helmi Suid[1], Mohd Zaidi Mohd Tumari[2]
[1]Faculty of Electrical and Electronics Engineering Technology, University Malaysia Pahang, Pahang
[2]Faculty of Electrical & Electronic Engineering Technology, Universiti Teknikal Malaysia Melaka, Melaka

Article Info

Article history:

ReceivedJun 9, 2016
Revised Nov 20, 2016
Accepted Dec 11, 2016

Keywords:

First keyword
Second keyword
Third keyword
Fourth keyword
Fifth keyword

ABSTRACT

This paper presents the identification of liquid slosh plant using the Hammerstein model based on Grey Wolf Optimizer (GWO) method. A remote car that carrying a container of liquid is considered as the liquid slosh experimental rig. In contrast to other research works, this paper consider a piece-wise affine function in the nonlinear function of the Hammerstein model, which is more generalized function. Moreover, a continuous-time transfer function is utilized in the Hammerstein model, which is more suitable to represent a real system. The GWO method is used to tune both coefficients in the nonlinear function and transfer function of the Hammerstein model such that the error between the identified output and the real experimental output is minimized. The effectiveness of the proposed framework is assessed in terms of the convergence curve response, output response, and the stability of the identified model through the bode plot and pole zero map. The results show that the GWO based method is able to produce a Hammerstein model that yields identified output response close to the real experimental slosh output.

Corresponding Author:

Mohd Ashraf Ahmad,
Faculty of Electrical and Electronics Engineering Technology,
University Malaysia Pahang, 26600, Pekan, Pahang, Malaysia.
Email: mashraf@ump.edu.my

1. INTRODUCTION

Nowadays, liquid slosh inside a cargo always happens in many situations. For example, ships with liquid container carriers are at high risk of generating sloshing load during operation [1]. In the metal industries, high oscillation can spill molten metal that is dangerous to the operator [2]. Meanwhile, sloshing of fuel and other liquids in moving vehicles may cause instability and undesired dynamics [3]. Hence, it is necessary to completely study the behavior of this residual slosh induced by the container motion. One may study the behavior of liquid slosh through developing the exact mathematical model of liquid slosh. So far, many researchers focus on the first principle approach to model the slosh behavior, while there are few literatures to discuss it from the perspective of nonlinear system identification approach.

On the other hand, block oriented nonlinear system identification has became a popular techniques to model a complex plants. The block oriented nonlinear model can be classified into three categories, which are Hammerstein model, Wiener model and Hammerstein Wiener model. In particular, Hammerstein model is a model that consists of a nonlinear function followed by linear dynamic sub-plant, while Wiener model consists of a linear dynamic sub-plant followed by nonlinear function, and finally, Hammerstein-Wiener model contains a linear dynamic sub-plant inserted between two or more nonlinear functions in series. Among these three block oriented models, Hammerstein model is famous due to its simple model structure and it has been widely used for nonlinear system identification. Specifically, the Hammerstein model has been applied to model a real plant such as Solid Oxide fuel cell [4], bidirectional DC motor [5], oxygen uptake estimation [6], stretch reflex dynamics [7], turntable servo system [8], pneumatic muscle actuators [9],

amplified piezoelectric actuators [10] and multi-axis piezoelectric micro positioning stages [11]. On the other hand, there are many tools that have been utilized to identify the Hammerstein model. There are the iterative method [12]-[14], the subspace method [15]-[17], the least square method [18], the blind approach [19] and the parametric instrumental variables method [20]. Moreover, many also consider the optimization tools for Hammerstein model, such as Bacterial Foraging algorithm [21], Cuckoo search algorithm [22], Particle Swarm optimization [23], and Genetic algorithm [24].

Based on the above literature, several limitations are ineluctable in their works, which are:

(i) Most of the Hammerstein models used in their study are based on discrete-time model, while many real plants can be easily represented in continuous-time model.

(ii) Almost all the methods assume a known structure of nonlinear function, which consists of several basis functions.

Though, our proposed work can solve a more general class of continuous-time Hammerstein model by assuming an unknown structure of nonlinear function. In particular, a piece-wise affine function is adopted with so many basis functions. Due to the introduction of the piece-wise affine function, a high dimensional design parameter tuning is considered in this study, which make the identification problem more complex. On the other hand, Grey Wolf Optimizer (GWO) [25] has become a top notch optimization algorithm which has solved various types of engineering problems [25]-[28]. To the best of our knowledge, there are still few works to discuss on the GWO for identification of Hammerstein model. Thence, it motivates us to see the effectiveness of the GWO in modeling the liquid slosh plant from the real experimental data.

This paper presents the identification of liquid slosh plant using the Hammerstein model based on GWO method. A remote car that carrying a container of liquid is considered as the liquid slosh experimental rig. The GWO method is used to tune both coefficients in the nonlinear function and transfer function of the Hammerstein model such that the error between the identified output and the real experimental output is minimized. The effectiveness of the proposed framework is assessed in terms of the convergence curve response, output response, and the stability of the identified model through the bode plot and pole zero map.

2. RESEARCH METHOD

This section explains on how the identification of liquid slosh based on Hammerstein model and GWO based method is performed. Firstly, the experimental setup of liquid slosh plant is explained. Here, it is shown on how the input and output data are generated. Secondly, we show the procedure to identify the model of liquid slosh plant using the Hammerstein based Grey Wolf Optimizer.

2.1. Liquid Slosh Experimental Rig

In this study, a mobile liquid slosh plant is considered to replicate real situation of a moving container carrying liquid, as shown in Figure 1. In particular, a remote control car is used to carry a small tank filled with liquid. The tank is also equipped with four plastic wheels so that it can move smoothly as shown in Figure 1(a). Moreover, three accelerometer sensors (ADXL335) that are floated on the surface of liquid are used to measure liquid oscillation as shown in Figure 1(b). For simplicity of our study, the liquid slosh data from only one of the sensor is recorded and only z-axis output data is considered. Figure 2 shows a general schematic diagram of liquid slosh experimental rig. In particular, an Arduino UNO is used as a data acquisition platform to process the input and output data. Here, we generate a voltage from the Arduino UNO to the remote car and concurrently the Arduino UNO also will acquire the slosh data from the accelerometer. Both the input and output data can be monitored and analyzed from the personal computer using the LabView software. In order to identify the model of liquid slosh, the remote car is required to move to a certain distance and suddenly stop to generate a liquid oscillation or slosh inside the tank. Thence, we apply the input voltage as shown in Figure 3 to move the remote car. Concurrently, the liquid slosh data is recorded as shown in Figure 4. These two data are then used to develop the Hammerstein model based GWO, which is discussed in the next section.

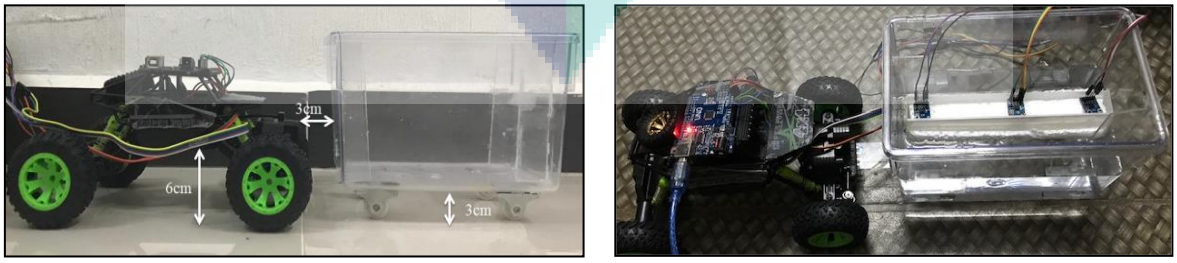

(a) Side view (b) Plan view

Figure 1. Liquid slosh experimental rig

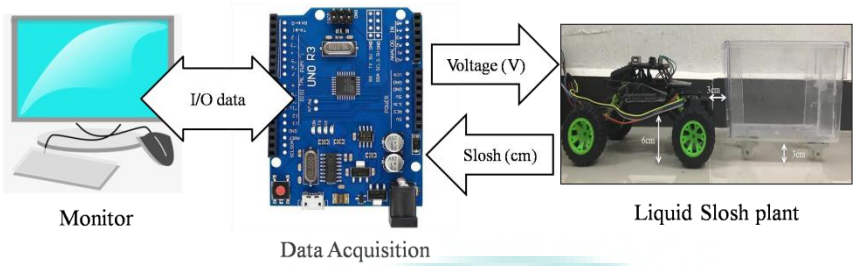

Figure 2. Schematic diagram of liquid slosh experimental rig

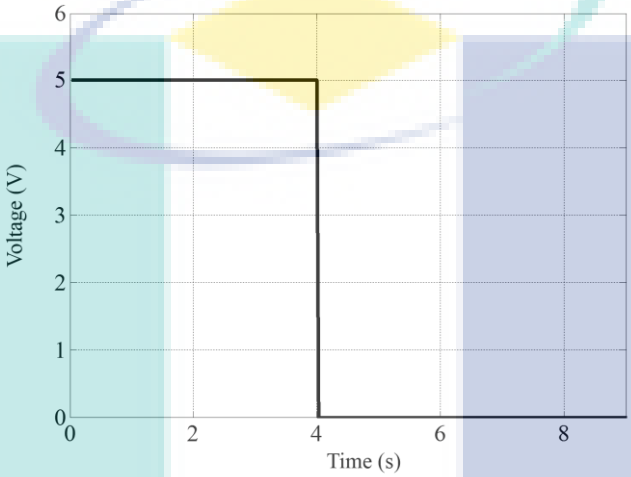

Figure 3. Input voltage applied to the remote car

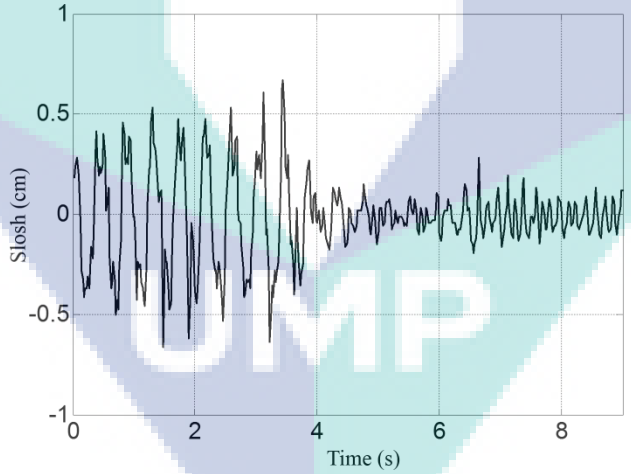

Figure 4. Output slosh from the accelerometer

2.2. Identification of Liquid Slosh using Hammerstein based Grey Wolf Optimizer

In this section, the proposed Grey Wolf Optimizer (GWO) for identification of liquid slosh plant in Section 2.1 based on Hammerstein model is presented. Firstly, a problem formulation to identify the liquid slosh plant is explained. Then, it is shown on how to apply the GWO method to identify the liquid slosh based on Hammerstein model.

Figure 5 shows a complete block diagram to identify the liquid slosh model in Section 2.1. The proposed Hammerstein model consists of nonlinear function $h(u)$ followed by the transfer function $G(s)$. The nonlinear function is a piece-wise affine function given by

$$h(u)=\begin{cases} c_0+m_1(u-d_0) & \text{if} \quad d_0 \le u < d_1, \\ c_1+m_2(u-d_1) & \text{if} \quad d_1 \le u < d_2, \\ \vdots & \\ c_{\sigma-1}+m_\sigma(u-d_{\sigma-1}) & \text{if} \quad d_{\sigma-1} \le u < d_\sigma, \end{cases} \tag{1}$$

and the transfer function $G(s)$ is given by

$$G(s)=\frac{B(s)}{A(s)}=\frac{s^m+b_{m-1}s^{m-1}+\cdots+b_0}{a_m s^m+a_{m-1}s^{m-1}+\cdots+a_0}. \tag{2}$$

In (1), the symbol $m_i=(c_i-c_{i-1})/(d_i-d_{i-1})(i=1,2,...,\sigma)$ are the segment slope with connecting input and output points as $d_i\,(i=0,1,...,\sigma)$ and $c_i\,(i=0,1,...,\sigma)$, respectively. For simplicity of notation, let $\boldsymbol{d}$ = [d_0, d_1, …, d_σ]^T and $\boldsymbol{c}$ = [c_0, c_1, …, c_σ]^T. The input of the real liquid slosh plant and the identified model is defined by $u(t)$, while the output of the real liquid slosh plant and the identified model are denoted by $y(t)$ and $\tilde{y}(t)$, respectively. Thence, the expression of the identified output can be written as

$$\tilde{y}(t)=G(s)h(u(t)). \tag{3}$$

Moreover, several assumptions are adopted in this work, which are:

(i) The order of the polynomial $A(s)$ and $B(s)$ are assumed to be known

(ii) The nonlinear function $h(u(t))$ is one-to-one map to the input $u(t)$ and the values of $d_i\,(i=1,2,...,\sigma)$ are pre-determined according to the response of input $u(t)$.

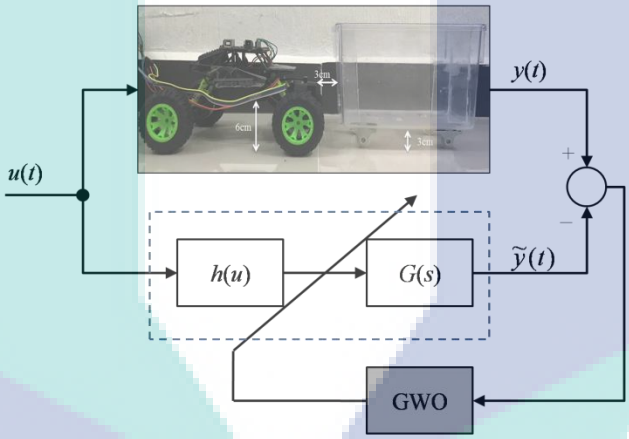

Figure 5. Block diagram of Hammerstein model based GWO

Next, let t_s be a sampling time for the real experimental input and output data ($u(t)$, $y(t)$) (t = 0, t_s, 2t_s, …, Nt_s). Then, in order to accurately identify the liquid slosh model, the following objective function in (4) is adopted in this study:

$$E(G,h)=\sum_{\eta=0}^{N}\left(y(\eta t_s)-\tilde{y}(\eta t_s)\right)^2. \tag{4}$$

Finally, our problem formulation can be described as follows.

Problem 1. Based on the given real experimental data ($u(t)$, $y(t)$) in Figure 1, find the nonlinear function $h(u)$ and the transfer function $G(s)$ such that the objective function in (4) is minimized.

Furthermore, it is shown on how to apply the GWO in solving **Problem 1**. For simplicity, let the design parameter of **Problem 1** is defined as $\boldsymbol{x}=\begin{bmatrix} b_0 & b_1 & \cdots & b_{m-1} & a_0 & a_1 & \cdots & a_m & c_0 & \cdots & c_\sigma \end{bmatrix}^T$, where the elements of the design parameter are the coefficients of both the nonlinear function and the transfer function of the continuous-time Hammerstein model. In GWO framework, let $\boldsymbol{x}_i\,(i=1,2,...,M)$ be the design parameter of each agent i for M total number of agents. Then, consider $x_{ij}\,(j=1,2,\ldots,D)$ be the j-th element of the vector $\boldsymbol{x}_i\,(i=1,2,...,M)$, where D is the size of the design parameter. Thence, by adopting objective function in (4), a minimization problem is expressed as

$$arg \min_{\boldsymbol{x}_i(1),\, \boldsymbol{x}_i(2),\ldots} E(\boldsymbol{x}_i(k)). \tag{5}$$

for iterations k = 1, 2, …, until maximum iteration $k_{\max}$. Finally, the procedure of the GWO in solving **Problem 1** is shown below:

Step 1: Determine the total number of agents M and the maximum iteration $k_{\max}$. Set k = 0 and initialize the design parameter $\boldsymbol{x}_i(0)(i=1,2,...,M)$ according to the upper bound $\boldsymbol{x}_{\text{up}}$ and lower bound $\boldsymbol{x}_{\text{low}}$ values of the design parameter.

Step 2: Calculate the objective function in (4) for each search agent i.

Step 3: Update the values of the best design parameter $\boldsymbol{x}^{\alpha}$, the second best design parameter $\boldsymbol{x}^{\beta}$ and the third best design parameter $\boldsymbol{x}^{\delta}$ based on the generated objective function in **Step 2**.

Step 4: For each agent, update the design parameter using the following equation:

$$\boldsymbol{x}_i(k+1) = \frac{\boldsymbol{x}^1 + \boldsymbol{x}^2 + \boldsymbol{x}^3}{3}, \tag{6}$$

where

$$\boldsymbol{x}^1 = \boldsymbol{x}^{\alpha} - \boldsymbol{P} \cdot \left| \boldsymbol{Q} \cdot \boldsymbol{x}^{\alpha} - \boldsymbol{x}_i(k) \right|,\ \boldsymbol{x}^2 = \boldsymbol{x}^{\beta} - \boldsymbol{P} \cdot \left| \boldsymbol{Q} \cdot \boldsymbol{x}^{\beta} - \boldsymbol{x}_i(k) \right|,\ \boldsymbol{x}^3 = \boldsymbol{x}^{\delta} - \boldsymbol{P} \cdot \left| \boldsymbol{Q} \cdot \boldsymbol{x}^{\delta} - \boldsymbol{x}_i(k) \right| \tag{7}$$

for i =1, 2, ..., M. In (6), the vectors $\boldsymbol{P}$ and $\boldsymbol{Q}$ are expressed as follows:

$$\boldsymbol{P} = 2\boldsymbol{a} \cdot \boldsymbol{r}_1 - \boldsymbol{a}, \tag{8}$$

$$\boldsymbol{Q} = 2 \cdot \boldsymbol{r}_2, \tag{9}$$

where $\boldsymbol{r}_1$ and $\boldsymbol{r}_2$ are the random vectors, where each element is generated independently from 0 to 1, and each element of $\boldsymbol{a}$ is linearly decreased from 2 to 0 over the course of iteration using the following equation:

$$a = 2\left(1 - \frac{k}{k_{\max}}\right). \tag{10}$$

Note that the vectors of $\boldsymbol{P}$ and $\boldsymbol{Q}$ in (8) and (9), which consists of random vectors $\boldsymbol{r}_1$ and $\boldsymbol{r}_2$, are generated independently between $\boldsymbol{x}^1$, $\boldsymbol{x}^2$ and $\boldsymbol{x}^3$.

Step 5: After the maximum iteration is achieved, record the best design parameter $\boldsymbol{x}^{\alpha}$ and obtained the continuous-time Hammerstein model in Figure 1. Otherwise, repeat **Step 2**.

3. RESULTS AND ANALYSIS

In this section, the effectiveness of the GWO based method for identifying the liquid slosh system using continuous-time Hammerstein model is demonstrated. In particular, the convergence curve response of the objective function in (4), the bode plot and pole-zero mapping of linear function and the plot of nonlinear function, will be presented and analyzed in this study.

Based on the experimental setup in Section 2.1, the input response $u(t)$ as shown in Figure 3 is applied to the liquid slosh plant, and the output response $y(t)$ is recorded as shown in Figure 4. Here, the input and output data are sampled at t_s = 0.02 for N = 450. In this study, the structure of $G(s)$ is selected as follows:

$$G(s) = \frac{B(s)}{A(s)} = \frac{s^3 + b_2 s^2 + b_1 s + b_0}{a_4 s^4 + a_3 s^3 + a_2 s^2 + a_1 s + a_0}. \tag{11}$$

after performing several preliminary testing on the given data ($u(t)$, $y(t)$). Meanwhile, the input points for piece-wise affine function of $h(u(t))$ are given by $\boldsymbol{d}$ = [0, 0.2, 0.4, 0.6, 0.8, 1, 2, 3, 4, 5]$^{\mathsf{T}}$. The design parameter $\boldsymbol{x} \in \boldsymbol{R}^{18}$ with its corresponding transfer function and nonlinear function is shown in Table 1. Next, the GWO algorithm is applied to tune the design parameter with initial values of design parameter are randomly selected between the upper bound $\boldsymbol{x}_{\text{up}}$ and lower bound $\boldsymbol{x}_{\text{low}}$ as shown in Table 1. Here, we choose the number of agents M = 40 with maximum iterations $k_{\max}$ = 5000.

Figure 6 shows the response of the objective function convergence after 5000 iterations to produce the best design parameter as shown in the final column of Table 1. It shows that the GWO based method is able to minimize the objective function in (4) and produce a quite close output response $y(t)$ as compared to the real output $\tilde{y}(t)$, which can be clearly seen in Figure 7. Note that the identified output response tends to yield high oscillation when input is injected to the system and it start to attenuate when the input is zero, which is quite similar to the response of real experimental output.

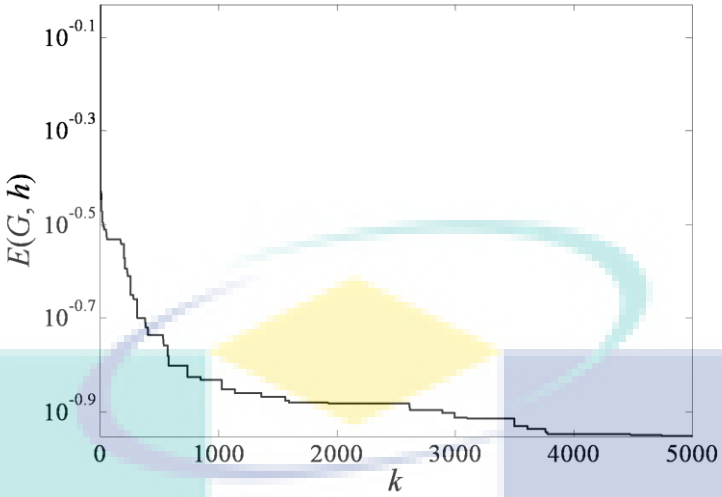

Figure 6. Convergence curve response

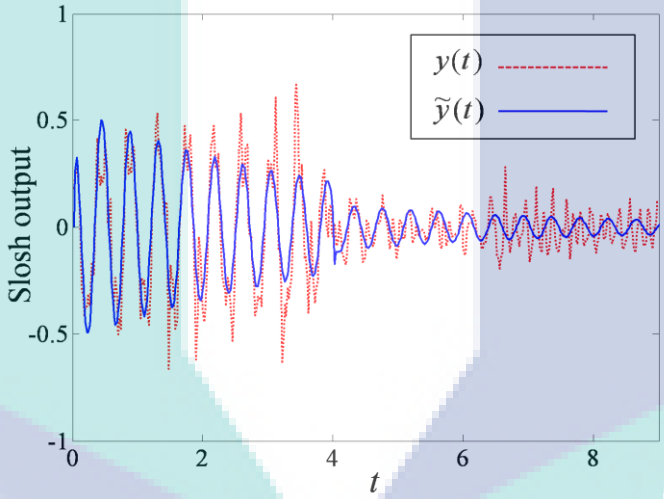

Figure 7. Response of the identified output $\tilde{y}(t)$ and real output $y(t)$

Table 1. Design parameter of liquid slosh plant

x	Coefficients	x_{low}	x_{up}	x^{α}
x_1	b_2	–5	35	–4.8017
x_2	b_1	–5	35	0.2657
x_3	b_0	–5	35	–0.0243
x_4	a_4	–5	35	–0.1119
x_5	a_3	–2200	–1	–4.3214
x_5	a_2	–2200	–1	–31.6384
x_7	a_1	–2200	–1	–901.2917
x_8	a_0	–2200	–1	–1280.4483
x_9	c_0	–5	5	–1.9997
x_{10}	c_1	–5	5	0.3249
x_{11}	c_2	–5	5	1.5968
x_{12}	c_3	–5	5	–0.0757
x_{13}	c_4	–5	5	–0.0099
x_{14}	c_5	–5	5	–0.0048
x_{15}	c_6	–5	5	–0.0251
x_{16}	c_7	–5	5	0.0584
x_{17}	c_8	–5	5	0.0216
x_{18}	c_9	–5	5	–2.2603

In the real experimental setup, we can say that the liquid slosh system is stable since the liquid slosh output is reduced gradually as $t \to \infty$. In order to validate our model regarding the stability, we use the bode diagram and the pole-zero map of the identified transfer function $G(s)$ as shown in Figures 8 and 9, respectively. From the bode diagram, it can be observed that a gain margin of 2.56 dB at 17.4 rad/s and phase margin of 4.18 degree at 16.5 rad/s are produced, which indicates that the linear system is stable. This is also supported by the pole-zero map where all the poles are located at the left hand side of y-axis. In particular, the obtained values of poles are –36.6623, –0.2344±j14.5053 and –1.4828, while the obtained values of zeros are 4.7468, 0.0274±j0.0661. On the other hand, we also can observe the feature of nonlinear function by plotting the obtained piece-wise function as depicted in Figure 10. Note that our nonlinear function is not restricted to any form of nonlinear function (i.e., quadratic), which is more generalized and provide more flexibility of searching a justifiable function.

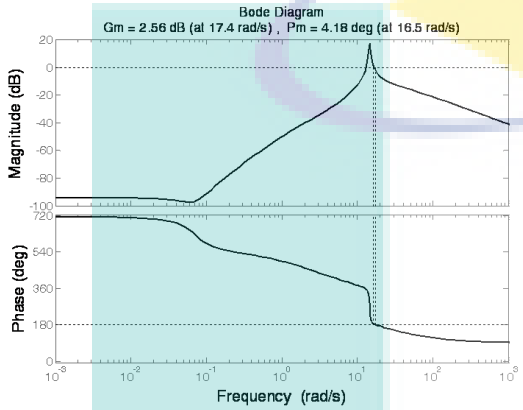

Figure 8. Bode plot of transfer function $G(s)$

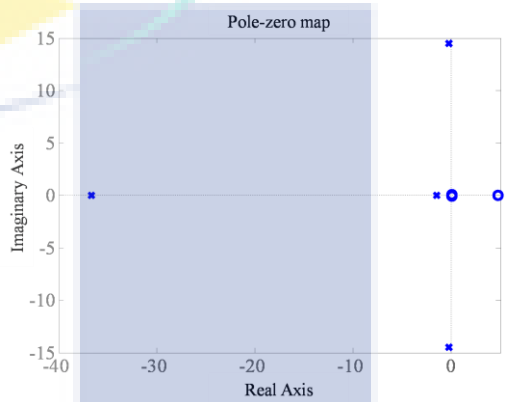

Figure 9. Pole-zero map of transfer function $G(s)$

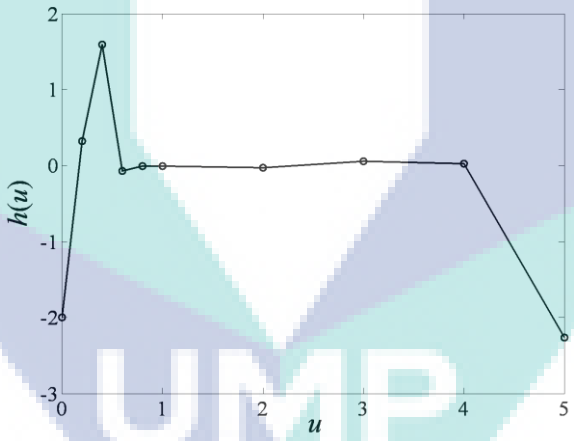

Figure 10. Resultant of piece-wise affine function $h(u)$

4. CONCLUSION

In this paper, an identification of liquid slosh plant using continuous-time Hammerstein model based on Grey Wolf Optimizer (GWO) has been presented. The results demonstrated that the proposed generic Hammerstein model based on GWO has a good potential in identifying the real liquid slosh behavior. In particular, it is shown that the proposed method is able to produce a quite close identified output with real liquid slosh output. Moreover, the resultant linear model has been proved to be stable based on the bode plot and pole-zero map. It is also shown that the used of piecewise-affine function gives more flexibility for the GWO to search more generic nonlinear function. In the future, our work can be extended to various types of nonlinear function such as continuous-time Wiener and Hammerstein-Wiener.

ACKNOWLEDGEMENTS

The authors gratefully acknowledged Research and Innovation Department of Universiti Malaysia Pahang under grant RDU1703153 for the financial support.

REFERENCES

[1] E. Rizzuto, R. Tedeschi, "Surveys of actual sloshing loads on board of ships at sea," *Proceedings of International Conference on Ship and Marine Research*, pp. 7.29-7.37, 1997.

[2] K. Terashima, G. Schmidt, "Sloshing analysis and suppression control of tilting-type automatic pouring machine," *Proceedings of IEEE International Symposium on Industrial Electronics*, pp. 275-280, 1994.

[3] T. Acarman, U. Ozguner, "Rollover prevention for heavy trucks using frequency shaped sliding mode control," *Vehicle System Dynamics*, vol. 44, no. 10, pp. 737-762, 2006.

[4] C. Li, *et al.*, "Identification of the Hammerstein model of a PEMFC stack based on least squares support vector machines," *Journal of Power Sources*, vol. 175, pp. 303-316, 2008.

[5] T. Kara, I. Eker, "Nonlinear modeling and identification of a DC motor for bidirectional operation with real time experiments," *Energy Conversion and Management*, vol. 45, no. 7-8, pp. 1087-1106, 2004.

[6] S.W. Su, *et al.*, "Oxygen uptake estimation in humans during exercise using a Hammerstein model," *Annals of biomedical engineering*, vol. 35, no. 11, pp. 1898-1906, 2007.

[7] D.T. Westwick, R.E. Kearney, "Separable least squares identification of nonlinear Hammerstein models: Application to stretch reflex dynamics," *Annals of Biomedical Engineering*, vol. 29, no. 8, pp. 707-718, 2001.

[8] Q. Zhang, *et al.*, "Nonlinear modeling and predictive functional control of Hammerstein system with application to the turntable servo system," *Mechanical Systems and Signal Processing*, vol. 72, pp. 383-394, 2016.

[9] Q. Ai, *et al.*, "Hammerstein model for hysteresis characteristics of pneumatic muscle actuators," *International Journal of Intelligent Robotics and Applications*, vol. 3, no. 1, pp. 33-44, 2019.

[10] A. Saleem, *et al.*, "Nonlinear hammerstein model identification of amplified piezoelectric actuators (APAs): Experimental considerations," *4th International Conference on Control, Decision and Information Technologies (CoDIT)*, pp. 0633-0638, 2017.

[11] H.T. Zhang, *et al.*, "Distributed Hammerstein Modeling for Cross-Coupling Effect of Multiaxis Piezoelectric Micropositioning Stages," *IEEE/ASME Transactions on Mechatronics*, vol. 23, no. 6, pp. 2794-2804, 2018.

[12] E.W. Bai, D. Li, "Convergence of the iterative Hammerstein system identification algorithm," *IEEE Transactions on automatic control*, vol. 49, no. 11, pp. 1929-1940, 2004.

[13] J. Hou, *et al.*, "Fixed point iteration-based subspace identification of Hammerstein state-space models," *IET Control Theory & Applications*, vol. 13, no. 8, pp. 1173-1181, 2019.

[14] Z. Ge, *et al.*, "Gradient-based iterative identification method for multivariate equation-error autoregressive moving average systems using the decomposition technique," *Journal of the Franklin Institute*, vol. 356, no. 3, pp. 1658-1676, 2019.

[15] J. Hou, *et al.*, "Subspace Hammerstein model identification under periodic disturbance," *IFAC-PapersOnLine*, vol. 51, no. 15, pp. 335-340, 2018.

[16] J. Hou, *et al.*, "Subspace identification of Hammerstein-type nonlinear systems subject to unknown periodic disturbance," *International Journal of Control*, (just-accepted), pp. 1-29, 2019.

[17] I.W. Jamaludin, N.A. Wahab, "Recursive Subspace Identification Algorithm using the Propagator Based Method," *Indonesian Journal of Electrical Engineering and Computer Science*, vol. 6, no. 1, pp. 172-179, 2017.

[18] D. Wang, W. Zhang, "Improved least squares identification algorithm for multivariable Hammerstein systems," *Journal of the Franklin Institute*, vol. 352, no. 11, pp. 5292-5307, 2015.

[19] E.W. Bai, "A blind approach to the Hammerstein–Wiener model identification," *Automatica*, vol. 38, no. 6, pp. 967-979, 2002.

[20] L. Ma, X. Liu, "A nonlinear recursive instrumental variables identification method of Hammerstein ARMAX system," *Nonlinear Dynamics*, vol. 79, no. 2, pp. 1601-1613, 2015.

[21] W. Lin, P.X. Liu, "Hammerstein model identification based on bacterial foraging," *Electronics Letters*, vol. 42, no. 23, pp. 1332-1333, 2006.

[22] A. Gotmare, *et al.*, "Nonlinear system identification using a cuckoo search optimized adaptive Hammerstein model," *Expert systems with applications*, vol. 42, no. 5, pp. 2538-2546, 2015.

[23] H.N. Al-Duwaish, "Identification of Hammerstein models with known nonlinearity structure using particle swarm optimization," *Arabian Journal for Science and Engineering*, vol. 36, no. 7, pp. 1269-1276, 2011.

[24] H. Zhang, H. Zhang, "Identification of Hammerstein Model Based on Quantum Genetic Algorithm", *Telkomnika*, vol. 11, no. 12, pp. 7206-7212, 2013.

[25] S. Mirjalili, *et al.*, "Grey wolf optimizer," *Advances in engineering software*, *69*, pp. 46-61, 2014.

[26] Y.L. Karnavas, *et al.*, "Permanent magnet synchronous motor design using grey wolf optimizer algorithm," *International Journal of Electrical and Computer Engineering*, vol. 6, no. 3, pp. 1353-1362, 2016.

[27] M.Z. Mohd Tumari, M.H. Suid, M.A. Ahmad, "A modified Grey Wolf Optimizer for improving wind plant energy production," *Indonesian Journal of Electrical Engineering and Computer Science*, Accepted, 2020.

[28] M.Z. Mohd Tumari, A.F. Zainal Abidin, A.A. Yusof, M.S. Mohd Aras, N.M.Z.A Mustapha, M.A. Ahmad, "Grey Wolf Optimizer fine-tuned model-free PID controller for depth control of hovering autonomous underwater vehicle," *Lecture Notes of Electrical Engineering*, Accepted, 2020.

Identification of Liquid Slosh Behavior using Continuous-time Hammerstein Model based Sine Cosine Algorithm

Julakha Jahan Jui[1], Mohd Helmi Suid[1], Zulkifli Musa[1], Mohd Ashraf Ahmad[1]

[1] Faculty of Electrical and Electronics Engineering Technology, University Malaysia Pahang, 26600, Pekan, Pahang, Malaysia
julakha.ump@gmail.com

Abstract. This paper presents the identification of liquid slosh plant using the Hammerstein model based on Sine Cosine Algorithm (SCA). A remote car that carrying a container of liquid is considered as the liquid slosh experimental rig. In contrast to other research works, this paper consider a piece-wise affine function in a nonlinear function of the Hammerstein model, which is more generalized function. Moreover, a continuous-time transfer function is utilized in the Hammerstein model, which is more suitable to represent a real system. The SCA method is used to tune both coefficients in the nonlinear function and the transfer function of the Hammerstein model such that the error between the identified output and the real experimental output is minimized. The effectiveness of the proposed framework is assessed in terms of the convergence curve response, output response, and the stability of the identified model through the pole-zero map. The results show that the SCA based method is able to produce a Hammerstein model that yields identified output response closes to the real experimental slosh output with 80.44 % improvement of sum of quadratic error.

Keywords: Slosh behavior, Sine Cosine Algorithm, Hammerstein model.

1 Introduction

Nowadays, liquid slosh inside a cargo always happens in many situations. For example, ships with liquid container carriers are at high risk of generating sloshing load during operation [1]. In the metal industries, high oscillation can spill molten metal that is dangerous to the operator [2]. Meanwhile, sloshing of fuel and other liquids in moving vehicles may cause instability and undesired dynamics [3]. Hence, it is necessary to completely study the behavior of this residual slosh induced by the container motion. One may study the behavior of liquid slosh through developing the exact mathematical model of liquid slosh. So far, many researchers focus on the first principle approach to model the slosh behavior, while there are few literatures to discuss it from the perspective of nonlinear system identification approach.

On the other hand, block oriented nonlinear system identification has became a popular techniques to model a complex plants. The block oriented nonlinear model

can be classified into three categories, which are Hammerstein model, Wiener model and Hammerstein Wiener model. In particular, Hammerstein model is a model that consists of a nonlinear function followed by linear dynamic sub-plant, while Wiener model consists of a linear dynamic sub-plant followed by nonlinear function, and finally, Hammerstein-Wiener model contains a linear dynamic sub-plant inserted between two or more nonlinear functions in series. Among these three block oriented models, Hammerstein model is famous due to its simple model structure and it has been widely used for nonlinear system identification. Specifically, the Hammerstein model has been applied to model a real plant such as Solid Oxide fuel cell [4], bidirectional DC motor [5], oxygen uptake estimation [6], stretch reflex dynamics [7], turntable servo system [8], pneumatic muscle actuators [9], amplified piezoelectric actuators [10] and multi-axis piezoelectric micro positioning stages [11]. On the other hand, there are many tools that have been utilized to identify the Hammerstein model. There are the iterative method [12]-[14], the subspace method [15]-[17], the least square method [18], the blind approach [19] and the parametric instrumental variables method [20]. Moreover, many also consider the optimization tools for Hammerstein model, such as Bacterial Foraging algorithm [21], Cuckoo search algorithm [22], Particle Swarm optimization [23], and Genetic algorithm [24].

Based on the above literature, several limitations are ineluctable in their works, which are:

(i) Most of the Hammerstein models used in their study are based on discrete-time model, while many real plants can be easily represented in continuous-time model.

(ii) Almost all the methods assume a known structure of nonlinear function, which consists of several basis functions.

Though, our proposed work can solve a more general class of continuous-time Hammerstein model by assuming an unknown structure of nonlinear function. In particular, a piece-wise affine function is adopted with so many basis functions. Due to the introduction of the piece-wise affine function, a high dimensional design parameter tuning is considered in this study, which make the identification problem more complex. On the other hand, Sine Cosine Algorithm (SCA) [25] has become a top notch optimization algorithm which has solved various types of engineering problems [25]-[27]. To the best of our knowledge, there are still few works to discuss on the SCA for identification of Hammerstein model. Moreover, other recent optimization methods are quite complex as compared to SCA which may contribute to high computation time in obtaining the result. Thence, it motivates us to see the effectiveness of the SCA in modeling the liquid slosh plant from the real experimental data.

This paper presents the identification of liquid slosh plant using the Hammerstein model based on SCA method. A remote car that carrying a container of liquid is considered as the liquid slosh experimental rig. The SCA method is used to tune both coefficients in the nonlinear function and transfer function of the Hammerstein model such that the error between the identified output and the real experimental output is minimized. The effectiveness of the proposed framework is assessed in terms of the convergence curve response, output response, and the stability of the identified model through the pole zero map.

2 Liquid Slosh Experimental Rig

In this study, a mobile liquid slosh plant is considered to replicate real situation of a moving container carrying liquid, as shown in Fig. 1. In particular, a remote control car is used to carry a small tank filled with liquid. The tank is also equipped with four plastic wheels so that it can move smoothly as shown in Fig. 1(a). Moreover, three accelerometer sensors (ADXL335) that are floated on the surface of liquid are used to measure liquid oscillation as shown in Fig. 1(b). For simplicity of our study, the liquid slosh data from only one of the sensor is recorded and only z-axis output data is considered. Fig. 2 shows a general schematic diagram of liquid slosh experimental rig. In particular, an Arduino UNO is used as a data acquisition platform to process the input and output data. Here, we generate a voltage from the Arduino UNO to the remote car and concurrently the Arduino UNO also will acquire the slosh data from the accelerometer. Both the input and output data can be monitored and analyzed from the personal computer using the LabView software. In order to identify the model of liquid slosh, the remote car is required to move to a certain distance and suddenly stop to generate a liquid oscillation or slosh inside the tank. Thence, we apply the input voltage as shown in Fig. 3 to move the remote car. Concurrently, the liquid slosh data is recorded as shown in Fig. 4. These two data are then used to develop the Hammerstein model based SCA, which is discussed in the next section.

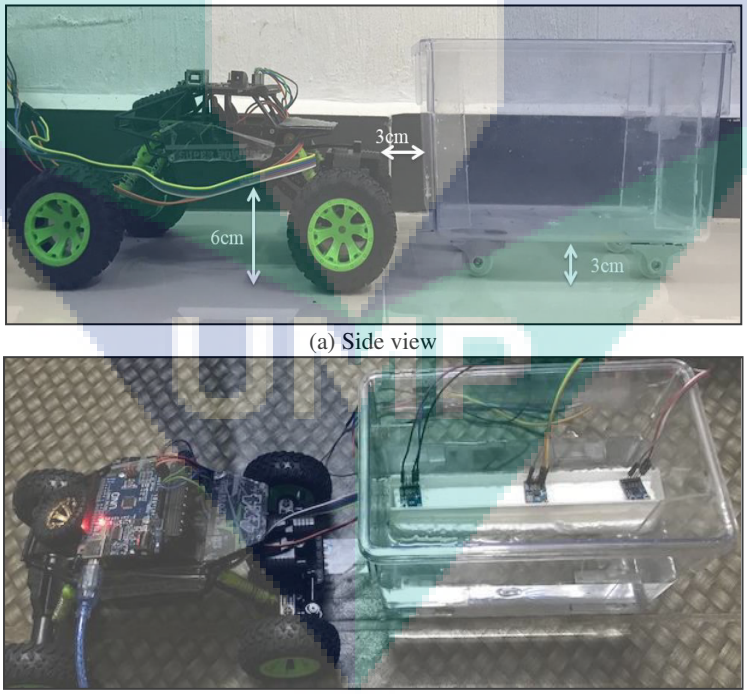

(a) Side view

(b) Plan view

Fig.1. Liquid slosh experimental rig

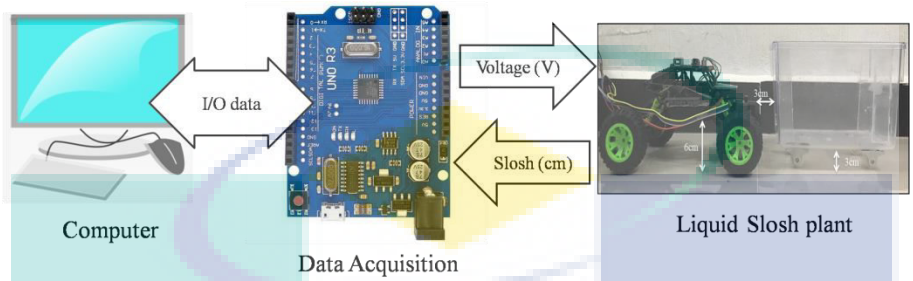

Fig.2. Schematic diagram of liquid slosh experimental rig

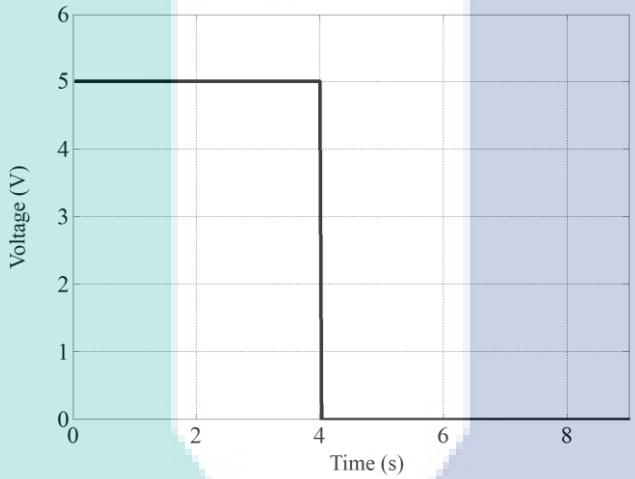

Fig.3. Input voltage applied to the remote car

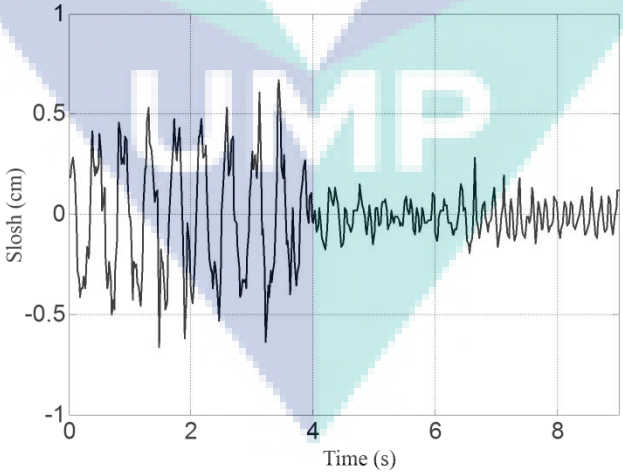

Fig.4. Output slosh from the accelerometer

3 Identification of Liquid Slosh using Hammerstein based SCA

In this section, the proposed Sine Cosine Algorithm (SCA) for identification of liquid slosh plant in Section 2 based on Hammerstein model is presented. Firstly, a problem formulation to identify the liquid slosh plant is explained. Then, it is shown on how to apply the SCA method to identify the liquid slosh based on Hammerstein model.

Fig. 5 shows a complete block diagram to identify the liquid slosh model in Section 2. The proposed Hammerstein model consists of nonlinear function $h(u)$ followed by the transfer function $G(s)$. The nonlinear function is a piece-wise affine function given by

$$h(u)=\begin{cases} c_0+m_1(u-d_0) & \text{if} \quad d_0 \le u < d_1, \\ c_1+m_2(u-d_1) & \text{if} \quad d_1 \le u < d_2, \\ \vdots & \\ c_{\sigma-1}+m_\sigma(u-d_{\sigma-1}) & \text{if} \quad d_{\sigma-1} \le u < d_\sigma, \end{cases} \tag{1}$$

and the transfer function $G(s)$ is given by

$$G(s)=\frac{B(s)}{A(s)}=\frac{s^m+b_{m-1}s^{m-1}+\cdots+b_0}{a_m s^m+a_{m-1}s^{m-1}+\cdots+a_0}. \tag{2}$$

In (1), the symbol $m_i=(c_i-c_{i-1})/(d_i-d_{i-1})(i=1,2,...,\sigma)$ are the segment slope with connecting input and output points as $d_i\,(i=0,1,...,\sigma)$ and $c_i\,(i=0,1,...,\sigma)$, respectively. For simplicity of notation, let $\boldsymbol{d}=[d_0, d_1, \ldots, d_\sigma]^\mathsf{T}$ and $\boldsymbol{c}=[c_0, c_1, \ldots, c_\sigma]^\mathsf{T}$. Note that the total number of input or output points are $\sigma+1$. The input of the real liquid slosh plant and the identified model is defined by $u(t)$, while the output of the real liquid slosh plant and the identified model are denoted by $y(t)$ and $\tilde{y}(t)$, respectively. Thence, the expression of the identified output can be written as

$$\tilde{y}(t)=G(s)h(u(t)). \tag{3}$$

Moreover, several assumptions are adopted in this work, which are:

(i) The order of the polynomial $A(s)$ and $B(s)$ are assumed to be known

(ii) The nonlinear function $h(u(t))$ is one-to-one map to the input $u(t)$ and the values of $d_i\,(i=1,2,...,\sigma)$ are pre-determined according to the response of input $u(t)$.

Next, let t_s be a sampling time for the real experimental input and output data ($u(t)$, $y(t)$) ($t=0, t_s, 2t_s, \ldots, Nt_s$). Then, in order to accurately identify the liquid slosh model, the following objective function in (4) is adopted in this study:

$$E(G,h)=\sum_{\eta=0}^{N}\left(y(\eta t_s)-\tilde{y}(\eta t_s)\right)^2. \tag{4}$$

Note that the objective function in (4) is based on the sum of quadratic error, which has been widely used in many literature [28]-[29]. Finally, our problem formulation can be described as follows.

Problem 1. Based on the given real experimental data ($u(t)$, $y(t)$) in Fig. 1, find the nonlinear function $h(u)$ and the transfer function $G(s)$ such that the objective function in (4) is minimized.

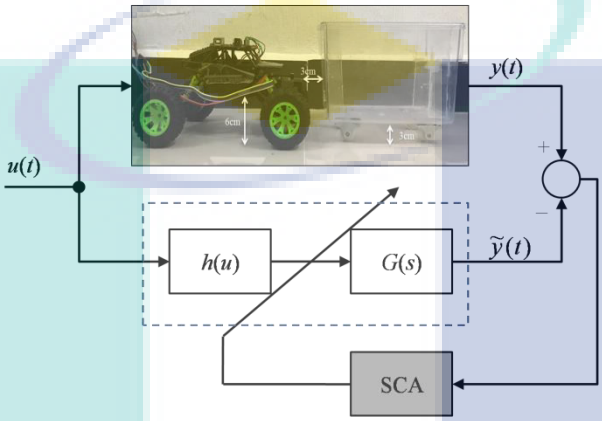

Fig.5. Block diagram of Hammerstein model based SCA

Furthermore, it is shown on how to apply the SCA in solving **Problem 1**. For simplicity, let the design parameter of **Problem 1** is defined as $\boldsymbol{x} = [b_0 \quad b_1 \quad \cdots \quad b_{m-1} \quad a_0 \quad a_1 \quad \cdots \quad a_m \quad c_0 \quad \cdots \quad c_\sigma]^{\mathrm{T}}$, where the elements of the design parameter are the coefficients of both the nonlinear function and the transfer function of the continuous-time Hammerstein model. In SCA framework, let $\boldsymbol{x}_i\,(i = 1, 2, ..., M)$ be the design parameter of each agent i for M total number of agents. Then, consider $x_{ij}\,(j = 1, 2, \ldots, D)$ be the j-th element of the vector $\boldsymbol{x}_i\,(i = 1, 2, ..., M)$, where D is the size of the design parameter. Thence, by adopting objective function in (4), a minimization problem is expressed as

$$arg \min_{\boldsymbol{x}_i(1),\, \boldsymbol{x}_i(2), \ldots} E(\boldsymbol{x}_i(k)). \tag{5}$$

for iterations k = 1, 2, …, until maximum iteration $k_{\max}$. Finally, the procedure of the SCA in solving **Problem 1** is shown as follows:

Step 1: Determine the total number of agents M and the maximum iteration $k_{\max}$. Set k = 0 and initialize the design parameter $\boldsymbol{x}_i(0)(i = 1, 2, ..., M)$ according to the upper bound $\boldsymbol{x}_{\mathrm{up}}$ and lower bound $\boldsymbol{x}_{\mathrm{low}}$ values of the design parameter.

Step 2: Calculate the objective function in (4) for each search agent i.

Step 3: Update the values of the best design parameter $\boldsymbol{P}$ based on the generated objective function in **Step 2**.

Step 4: For each agent, update the design parameter using the following equation:

$$x_{ij}(k+1)=\begin{cases} x_{ij}(k)+r_1\sin(r_2)\times\left\|r_3P_j-x_{ij}(k)\right\| & \text{if} \quad r_4<0.5, \\ x_{ij}(k)+r_1\cos(r_2)\times\left\|r_3P_j-x_{ij}(k)\right\| & \text{if} \quad r_4\geq 0.5, \end{cases} \tag{6}$$

where

$$r_1=2\left(1-\frac{k}{k_{\max}}\right) \tag{7}$$

for maximum iteration $k_{\max}$. Note that r_2, r_3 and r_4 are random values that are generated independently and uniformly in the ranges [0, 2π], [0, 2] and [0, 1], respectively. The detailed justification on the selection of the coefficients r_1, r_2, r_3 and r_4 are clearly explained in [25]. In (6), the symbol P_j (j = 1, 2, ..., n) is denoted as the best current design parameter in j-th element of $\boldsymbol{P}$ that is kept during tuning process.

Step 5: After the maximum iteration is achieved, record the best design parameter $\boldsymbol{P}$ and obtained the continuous-time Hammerstein model in Fig. 1. Otherwise, repeat **Step 2**.

4 Results and Analysis

In this section, the effectiveness of the SCA based method for identifying the liquid slosh system using continuous-time Hammerstein model is demonstrated. In particular, the convergence curve response of the objective function in (4), the pole-zero mapping of linear function and the plot of nonlinear function, will be presented and analyzed in this study.

Based on the experimental setup in Section 2, the input response $u(t)$ as shown in Fig. 3 is applied to the liquid slosh plant, and the output response $y(t)$ is recorded as shown in Fig. 4. Here, the input and output data are sampled at t_s = 0.02 s for N = 450. In this study, the structure of $G(s)$ is selected as follows:

$$G(s)=\frac{B(s)}{A(s)}=\frac{s^3+b_2s^2+b_1s+b_0}{a_4s^4+a_3s^3+a_2s^2+a_1s+a_0}. \tag{8}$$

after performing several preliminary testing on the given data ($u(t)$, $y(t)$). The fourth order system is used by considering a cascade of 2$^{\text{nd}}$ order system for both dc motor of remote car and the slosh dynamic. Meanwhile, the input points for piece-wise affine function of $h(u(t))$ are given by $\boldsymbol{d}$ = [0, 0.2, 0.4, 0.6, 0.8, 1, 2, 3, 4, 5]$^{\text{T}}$. The selection of vector $\boldsymbol{d}$ is obtained after several preliminary experiments. The design parameter $\boldsymbol{x}\in\boldsymbol{R}^{18}$ with its corresponding transfer function and nonlinear function is shown in Table 1. Next, the SCA algorithm is applied to tune the design parameter with initial values of design parameter are randomly selected between the upper bound $\boldsymbol{x}_{\text{up}}$ and lower bound $\boldsymbol{x}_{\text{low}}$ as shown in Table 1. Note that the values $\boldsymbol{x}_{\text{up}}$ and $\boldsymbol{x}_{\text{low}}$ are obtained after performing several preliminary experiments. Here, we choose the number of agents M = 40 with maximum iterations $k_{\max}$ = 5000.

Fig. 6 shows the response of the objective function convergence with the value of $E(G,h)$ = 0.1616 at $k_{\max}$ = 5000 with 80.44 % of objective function improvement to

produce the best design parameter ***P*** as shown in the final column of Table 1. It shows that the SCA based method is able to minimize the objective function in (4) and produce a quite close output response $y(t)$ as compared to the real output $\tilde{y}(t)$, which can be clearly seen in Fig. 7. Note that the identified output response tends to yield high oscillation when input is injected to the system and it start to attenuate when the input is zero, which is quite similar to the response of real experimental output.

In the real experimental setup, we can say that the liquid slosh system is stable since the liquid slosh output is reduced gradually as $t \to \infty$. In order to validate our model regarding the stability, we use the pole-zero map of the identified transfer function $G(s)$ as shown in Fig. 8. From the pole-zero map, all the poles are located at the left hand side of y-axis. In particular, the obtained values of poles are $-0.1190 \pm j14.8001$, -7.5621 and -0.8229, while the obtained values of zeros are 0.0872 and $1.8538 \pm j2.6373$. On the other hand, we also can observe the feature of nonlinear function by plotting the obtained piece-wise function as depicted in Fig. 9. Note that our nonlinear function is not restricted to any form of nonlinear function (i.e., quadratic), which is more generalized and provide more flexibility of searching a justifiable function.

Table 1. Design parameter of liquid slosh plant

$\boldsymbol{x}$	Coefficients	$\boldsymbol{x}_{\text{low}}$	$\boldsymbol{x}_{\text{up}}$	$\boldsymbol{P}$
x_1	b_2	–5	35	–3.7948
x_2	b_1	–5	35	10.7153
x_3	b_0	–5	35	–0.9059
x_4	a_4	–5	35	–0.6154
x_5	a_3	–2200	–1	–5.3112
x_5	a_2	–2200	–1	–139.8711
x_7	a_1	–2200	–1	–1132.2883
x_8	a_0	–2200	–1	–839.7621
x_9	c_0	–5	5	–4.8859
x_{10}	c_1	–5	5	–0.0219
x_{11}	c_2	–5	5	3.3211
x_{12}	c_3	–5	5	–4.7295
x_{13}	c_4	–5	5	–0.3240
x_{14}	c_5	–5	5	–4.4858
x_{15}	c_6	–5	5	-0.0002
x_{16}	c_7	–5	5	0.0000
x_{17}	c_8	–5	5	0.1679
x_{18}	c_9	–5	5	–4.3282

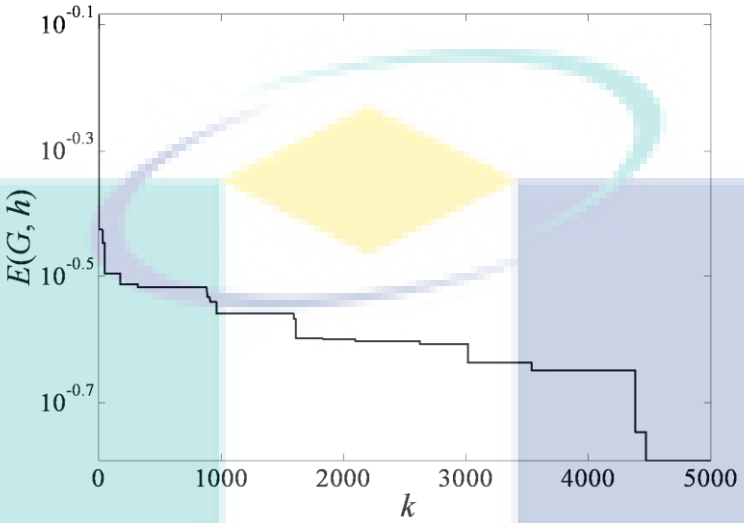

Fig.6. Convergence curve response

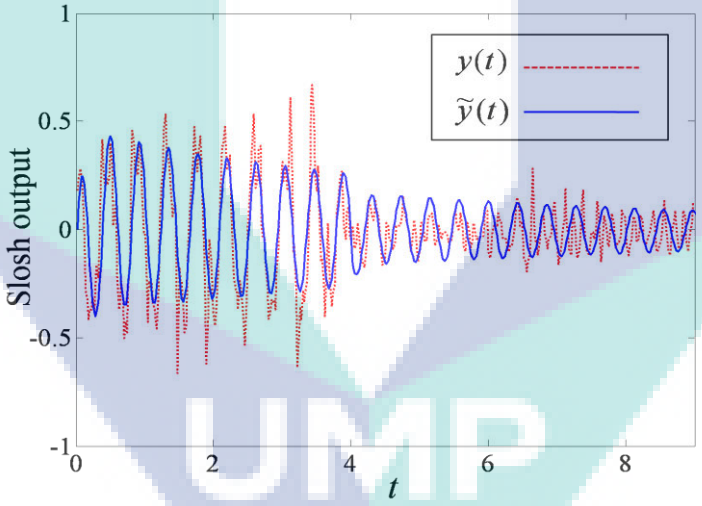

Fig.7. Response of the identified output $\tilde{y}(t)$ and real output $y(t)$

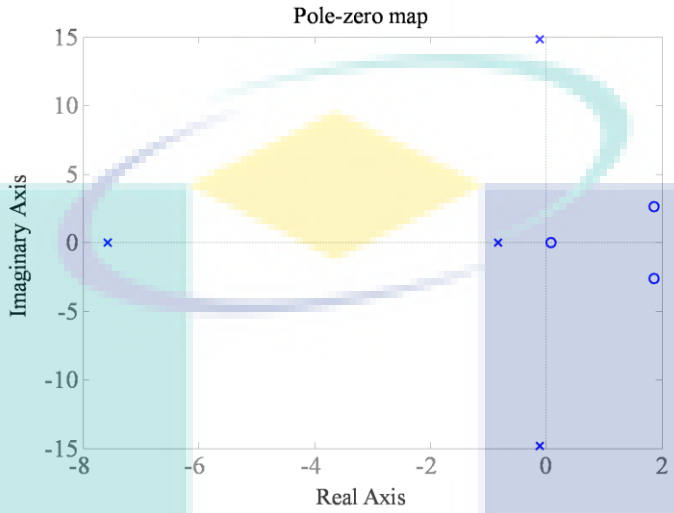

Fig.8. Pole-zero map of transfer function $G(s)$

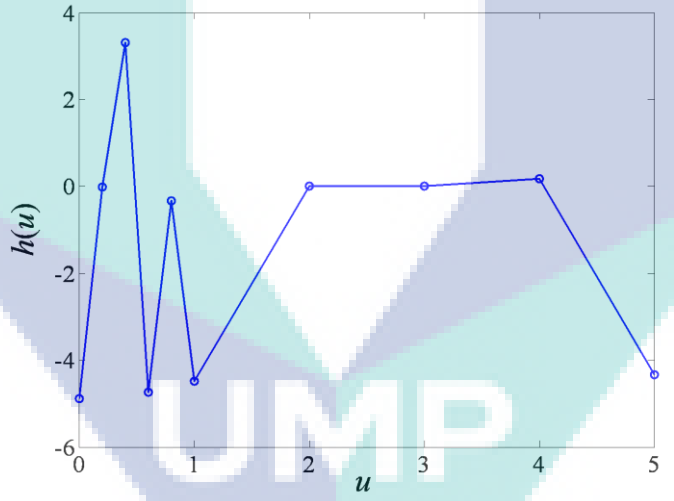

Fig.9. Resultant of piece-wise affine function $h(u)$

5 Conclusion

In this paper, an identification of liquid slosh plant using continuous-time Hammerstein model based on Sine Cosine Algorithm (SCA) has been presented. The results demonstrated that the proposed generic Hammerstein model based on SCA has a good potential in identifying the real liquid slosh behavior. In particular, it is shown

that the proposed method is able to produce a quite close identified output with real liquid slosh output. Moreover, the resultant linear model has been proved to be stable based on the pole-zero map. It is also shown that the used of piecewise-affine function gives more flexibility for the SCA to search more generic nonlinear function. In the future, our work can be extended to various types of nonlinear function such as continuous-time Wiener and Hammerstein-Wiener.

Acknowledgement

The authors gratefully acknowledged Research and Innovation Department of Universiti Malaysia Pahang under grant RDU1703153 for the financial support.

References

1. Rizzuto, E., Tedeschi, R.: Surveys of actual sloshing loads on board of ships at sea. In: Proceedings of International Conference on Ship and Marine Research, pp. 7.29-7.37, (1997).
2. Terashima, K., Schmidt, G.: Sloshing analysis and suppression control of tilting-type automatic pouring machine. In: Proceedings of IEEE International Symposium on Industrial Electronics, pp. 275-280 (1994).
3. Acarman, T., Ozguner, U.: Rollover prevention for heavy trucks using frequency shaped sliding mode control. Vehicle System Dynamics 44(10), 737-762 (2006).
4. Li,C., Zhu, X., Cao, G., Sui, S., Hu, M.: Identification of the Hammerstein model of a PEMFC stack based on least squares support vector machines. Journal of Power Sources 175, 303-316 (2008).
5. Kara, T., Eker, I.: Nonlinear modeling and identification of a DC motor for bidirectional operation with real time experiments. Energy Conversion and Management 45(7-8), 1087-1106 (2004).
6. Su, S.W., Wang, L. Celler, B.G., Savkin, A.V.: Oxygen uptake estimation in humans during exercise using a Hammerstein model. Annals of biomedical engineering 35(11), 1898-1906 (2007).
7. Westwick, D.T., Kearney, R.E.: Separable least squares identification of nonlinear Hammerstein models: Application to stretch reflex dynamics. Annals of Biomedical Engineering 29(8), 707-718 (2001).
8. Zhang, Q., Wang, Q., Li, G.: Nonlinear modeling and predictive functional control of Hammerstein system with application to the turntable servo system. Mechanical Systems and Signal Processing 72, 383-394 (2016).
9. Ai, Q., Peng, Y., Zuo, J., Meng, W., Liu, Q.: Hammerstein model for hysteresis characteristics of pneumatic muscle actuators. International Journal of Intelligent Robotics and Applications 3(1), 33-44 (2019).
10. Saleem, A., Mesbah, M., Al-Ratout, S.: Nonlinear Hammerstein model identification of amplified piezoelectric actuators (APAs): Experimental considerations. In 2017 4th International Conference on Control, Decision and Information Technologies (CoDIT), pp. 0633-0638 (2017).
11. Zhang, H.T., Hu, B., Li, L., Chen, Z., Wu, D., Xu, B., Huang, X., Gu, G., Yuan, Y.: Distributed Hammerstein Modeling for Cross-Coupling Effect of Multiaxis Piezoelectric Mi-

cropositioning Stages. In: IEEE/ASME Transactions on Mechatronics 23(6), 2794-2804 (2018).
12. Bai, E.W., Li, D.: Convergence of the iterative Hammerstein system identification algorithm. IEEE Transactions on automatic control 49(11), 1929-1940 (2004).
13. Hou, J., Chen, F., Li, P., Zhu, Z.: Fixed point iteration-based subspace identification of Hammerstein state-space models. IET Control Theory & Applications 13(8), 1173-1181 (2019).
14. Ge, Z., Ding, F., Xu, L., Alsaedi, A., Hayat, T.: Gradient-based iterative identification method for multivariate equation-error autoregressive moving average systems using the decomposition technique. Journal of the Franklin Institute 356(3), 1658-1676 (2019).
15. Hou, J., Liu, T., Wahlberg, B., Jansson, M.: Subspace Hammerstein model identification under periodic disturbance. IFAC-PapersOnLine, 51(15), 335-340 (2018).
16. Hou, J., Liu, T., Wang, Q.G.: Subspace identification of Hammerstein-type nonlinear systems subject to unknown periodic disturbance. International Journal of Control, (just-accepted), 1-29 (2019).
17. Jamaludin, I.W., Wahab, N.A.: Recursive Subspace Identification Algorithm using the Propagator Based Method. Indonesian Journal of Electrical Engineering and Computer Science 6(1), 172-179 (2017).
18. Wang, D., Zhang, W.: Improved least squares identification algorithm for multivariable Hammerstein systems. Journal of the Franklin Institute 352(11), 5292-5307 (2015).
19. Bai, E.W.: A blind approach to the Hammerstein–Wiener model identification. Automatica 38(6), 967-979 (2002).
20. Ma, L., Liu, X.: A nonlinear recursive instrumental variables identification method of Hammerstein ARMAX system. Nonlinear Dynamics 79(2), 1601-1613 (2015).
21. Lin, W., Liu, P.X.: Hammerstein model identification based on bacterial foraging. Electronics Letters 42(23), 1332-1333 (2006).
22. Gotmare, A., Patidar, R., George, N.V.: Nonlinear system identification using a cuckoo search optimized adaptive Hammerstein model. Expert systems with applications 42(5), 2538-2546 (2015).
23. Al-Duwaish, H.N.: Identification of Hammerstein models with known nonlinearity structure using particle swarm optimization. Arabian Journal for Science and Engineering 36(7), 1269-1276 (2011).
24. Zhang, H., Zhang, H.: Identification of Hammerstein Model Based on Quantum Genetic Algorithm. Telkomnika 11(12), 7206-7212 (2013).
25. Mirjalili, S.: SCA: a sine cosine algorithm for solving optimization problems. Knowledge-Based Systems 96, 120-133 (2016).
26. Suid, M.H., Tumari, M.Z. and Ahmad, M.A.: A modified sine cosine algorithm for improving wind plant energy production. Indonesian Journal of Electrical Engineering and Computer Science 16(1), 101-106 (2019).
27. Suid, M.H., Ahmad, M.A., Ismail, M.R.T.R., Ghazali, M.R., Irawan, A. and Tumari, M.Z.: An Improved Sine Cosine Algorithm for Solving Optimization Problems. In: IEEE Conference on Systems, Process and Control (ICSPC), pp. 209-213 (2018).
28. Mjahed, M. and Ayad, H.: Quadrotor Identification through the Cooperative Particle Swarm Optimization-Cuckoo Search Approach. Computational intelligence and neuroscience, 2019, 1-10 (2019).
29. Gupta, S., Gupta, R. and Padhee, S.: Parametric system identification and robust controller design for liquid–liquid heat exchanger system. IET Control Theory & Applications 12(10), 1474-1482 (2018).

Modified Sine Cosine Algorithm for Identification of Liquid Slosh based on Continuous-time Hammerstein Model

Julakha Jahan Jui[1], Mohd Helmi Suid[1], Mohd Riduwan Ghazali[1], Mohd Ashraf Ahmad[1], Mohd Zaidi Mohd Tumari[2]

[1]Faculty of Electrical and Electronics Engineering Technology, University Malaysia Pahang, 26600, Pekan, Pahang, Malaysia.
[2]Faculty of Electrical & Electronic Engineering Technology, Universiti Teknikal Malaysia Melaka, Melaka

Abstract. This paper presents the identification of liquid slosh plant using the Hammerstein model based on modified Sine Cosine Algorithm (mSCA). A remote car that carrying a container of liquid is considered as the liquid slosh experimental rig. In contrast to other research works, this paper considers a piece-wise affine function in a nonlinear function of the Hammerstein model, which is more generalized function. Moreover, a continuous-time transfer function is utilized in the Hammerstein model, which is more suitable to represent a real system. The mSCA method is used to tune both coefficients in the nonlinear function and the transfer function of the Hammerstein model such that the error between the identified output and the real experimental output is minimized. The effectiveness of the proposed framework is assessed in terms of the convergence curve response, output response, and the stability of the identified model through the pole-zero map. The results show that the mSCA based method is able to produce a Hammerstein model that yields identified output response closes to the real experimental slosh output with 82.12 % improvement of sum of quadratic error.

1. Introduction

Nowadays, liquid slosh inside a cargo always happens in many situations. For example, ships with liquid container carriers are at high risk of generating sloshing load during operation [1]. In the metal industries, high oscillation can spill molten metal that is dangerous to the operator [2]. Meanwhile, sloshing of fuel and other liquids in moving vehicles may cause instability and undesired dynamics [3]. Hence, it is necessary to completely study the behavior of this residual slosh induced by the container motion. One may study the behavior of liquid slosh through developing the exact mathematical model of liquid slosh. So far, many researchers focus on the first principle approach to model the slosh behavior, while there are few literatures to discuss it from the perspective of nonlinear system identification approach.

On the other hand, block oriented nonlinear system identification has becomepopular techniques to model a complex plant. The block oriented nonlinear model can be classified into three categories, which are Hammerstein model, Wiener model and Hammerstein Wiener model. In particular, Hammerstein model is a model that consists of a nonlinear function followed by linear dynamic sub-plant, while Wiener model consists of a linear dynamic sub-plant followed by nonlinear function, and finally, Hammerstein-Wiener model contains a linear dynamic sub-plant inserted between two or more nonlinear functions in series. Among these three block oriented models, Hammerstein model is famous due to its simple model structure and it has been widely used for nonlinear system identification. Specifically, the Hammerstein model has been applied to model a real plant such as

Solid Oxide fuel cell [4], bidirectional DC motor [5], oxygen uptake estimation [6], stretch reflex dynamics [7], turn-table servo system [8], pneumatic muscle actuators [9], amplified piezoelectric actuators [10] and multi-axis piezoelectric micro positioning stages [11]. On the other hand, there are many tools that have been utilized to identify the Hammerstein model. There are the iterative method [12]-[14], the subspace method [15]-[17], the least square method [18], the blind approach [19] and the parametric instrumental variables method [20]. Moreover, many also consider the optimization tools for Hammerstein model, such as Bacterial Foraging algorithm [21], Cuckoo search algorithm [22], Particle Swarm optimization [23] and Genetic algorithm [24].

Based on the above literature, several limitations are ineluctable in their works, which are:

(i) Most of the Hammerstein models used in their study are based on discrete-time model, while many real plants can be easily represented in continuous-time model.

(ii) Almost all the methods assume a known structure of nonlinear function, which consists of several basis functions.

Though, our proposed work can solve a more general class of continuous-time Hammerstein model by assuming an unknown structure of nonlinear function. In particular, a piece-wise affine function is adopted with so many basis functions. Due to the introduction of the piece-wise affine function, a high dimensional design parameter tuning is considered in this study, which make the identification problem more complex. On the other hand, Sine Cosine Algorithm (SCA) [25] has become a top notch optimization algorithm which has solved various types of engineering problems [25]-[27]. To the best of our knowledge, there are still few works to discuss on the SCA for identification of Hammerstein model. Moreover, other recent optimization methods are quite complex as compared to SCA which may contribute to high computation time in obtaining the result. Thence, it motivates us to see the effectiveness of the SCA in modelling the liquid slosh plant from the real experimental data. Moreover, based on our preliminary works on this problem, the standard SCA is still not able to provide high accuracy of liquid slosh model. Therefore, it motivates us to modify the standard SCA algorithm such that a better accuracy of liquid slosh plant can be obtained.

This paper presents the identification of liquid slosh plant using the Hammerstein model based on modified SCA (mSCA) method in [26]. A remote car that carrying a container of liquid is considered as the liquid slosh experimental rig. The mSCA method is used to tune both coefficients in the nonlinear function and transfer function of the Hammerstein model such that the error between the identified output and the real experimental output is minimized. The effectiveness of the proposed framework is assessed in terms of the convergence curve response, output response, and the stability of the identified model through the pole zero map.

2. Liquid Slosh Experimental Rig

In this study, a mobile liquid slosh plant is considered to replicate real situation of a moving container carrying liquid, as shown in figure 1. In particular, a remote control car is used to carry a small tank filled with liquid. The tank is also equipped with four plastic wheels so that it can move smoothly as shown in figure 1(a). Moreover, three accelerometer sensors (ADXL335) that are floated on the surface of liquid are used to measure liquid oscillation as shown in figure 1(b). For simplicity of our study, the liquid slosh data from only one of the sensor is recorded and only z-axis output data is considered. Figure 2 shows a general schematic diagram of liquid slosh experimental rig. In particular, an Arduino UNO is used as a data acquisition platform to process the input and output data. Here, we generate a voltage from the Arduino UNO to the remote car and concurrently the Arduino UNO also will acquire the slosh data from the accelerometer. Both the input and output data can be monitored and analysed from the personal computer using the LabVIEW software. In order to identify the model of liquid slosh, the remote car is required to move to a certain distance and suddenly stop to generate a liquid oscillation or slosh inside the tank. Thence, we apply the input voltage as shown in figure 3 to move the remote car. Concurrently, the liquid slosh data is recorded as shown in figure 4. These two data are then used to develop the Hammerstein model based SCA, which is discussed in the next section.

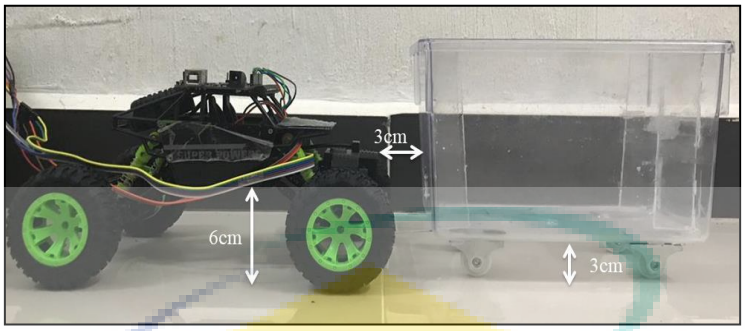

(a)

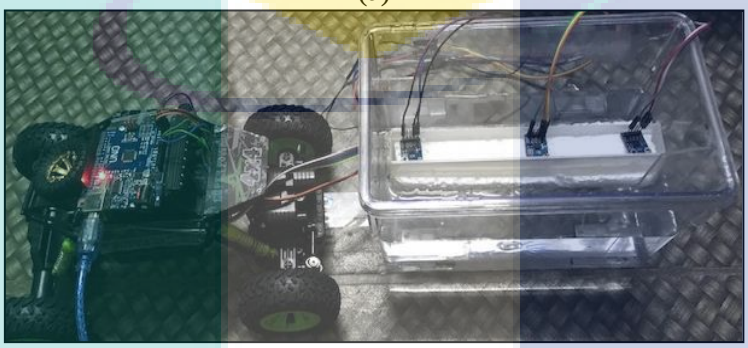

(b)

Figure 1. Liquid slosh experimental rig

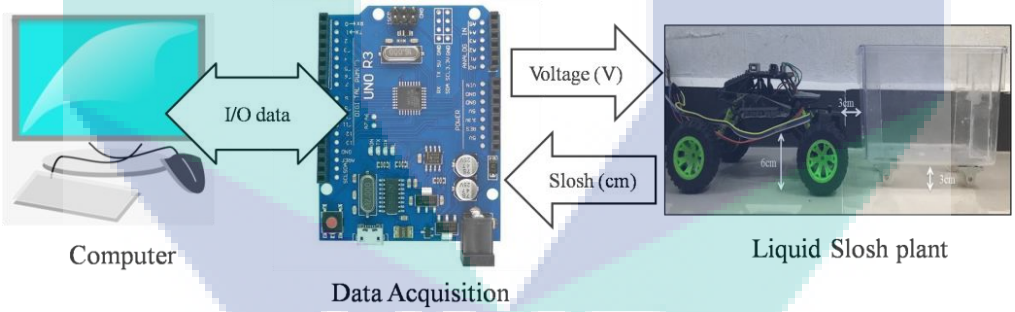

Figure 2. Schematic diagram of liquid slosh experimental rig

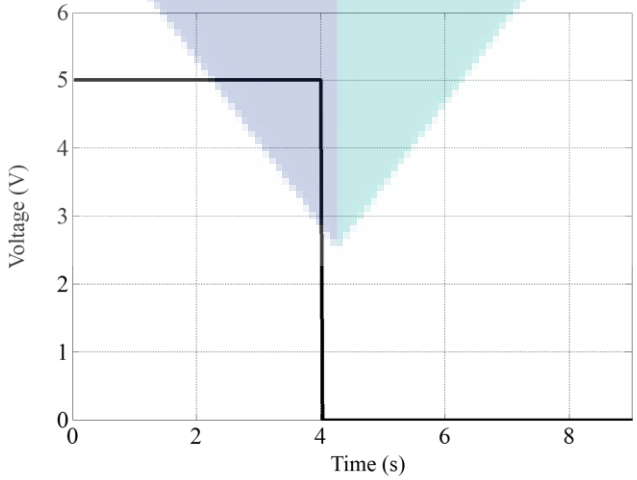

Figure 3. Input voltage applied to the remote car

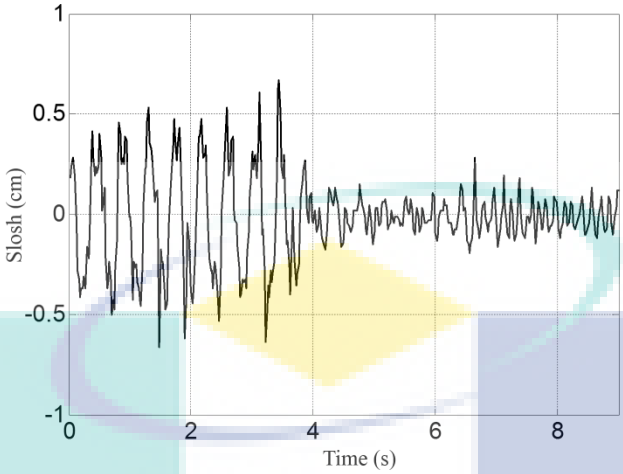

Figure 4. Output slosh from the accelerometer

3. Identification of Liquid Slosh using Hammerstein based modified SCA

In this section, the proposed modified Sine Cosine Algorithm (mSCA) for identification of liquid slosh plant in Section 2 based on Hammerstein model is presented. Firstly, a problem formulation to identify the liquid slosh plant is explained. Then, it is shown on how to apply the mSCA method to identify the liquid slosh based on Hammerstein model.

Figure 5 shows a complete block diagram to identify the liquid slosh model in Section 2. The proposed Hammerstein model consists of nonlinear function $h(u)$ followed by the transfer function $G(s)$. The nonlinear function is a piece-wise affine function given by

$$h(u) = \begin{cases} c_0 + m_1(u - d_0) & \text{if} \quad d_0 \le u < d_1, \\ c_1 + m_2(u - d_1) & \text{if} \quad d_1 \le u < d_2, \\ \vdots & \\ c_{\sigma-1} + m_\sigma(u - d_{\sigma-1}) & \text{if} \quad d_{\sigma-1} \le u < d_\sigma, \end{cases} \tag{1}$$

and the transfer function $G(s)$ is given by

$$G(s) = \frac{B(s)}{A(s)} = \frac{s^m + b_{m-1}s^{m-1} + \cdots + b_0}{a_m s^m + a_{m-1}s^{m-1} + \cdots + a_0}. \tag{2}$$

In (1), the symbol $m_i = (c_i - c_{i-1})/(d_i - d_{i-1})(i = 1, 2, ..., \sigma)$ are the segment slope with connecting input and output points as $d_i\ (i = 0, 1, ..., \sigma)$ and $c_i\ (i = 0, 1, ..., \sigma)$, respectively. For simplicity of notation, let $\boldsymbol{d} = [d_0, d_1, \ldots, d_\sigma]^T$ and $\boldsymbol{c} = [c_0, c_1, \ldots, c_\sigma]^T$. Note that the total number of input or output points are σ +1. The input of the real liquid slosh plant and the identified model is defined by $u(t)$, while the output of the real liquid slosh plant and the identified model are denoted by $y(t)$ and $\tilde{y}(t)$, respectively. Thence, the expression of the identified output can be written as

$$\tilde{y}(t) = G(s)h(u(t)) \tag{3}$$

Moreover, several assumptions are adopted in this work, which are:

(i) The order of the polynomial $A(s)$ and $B(s)$ are assumed to be known.

(ii) The nonlinear function $h(u(t))$ is one-to-one map to the input $u(t)$ and the values of $d_i\ (i=1,2,...,\sigma)$ are pre-determined according to the response of input $u(t)$.

Next, let t_s be a sampling time for the real experimental input and output data ($u(t)$, $y(t)$) (t = 0, t_s, 2t_s, …, Nt_s). Then, in order to accurately identify the liquid slosh model, the following objective function in (4) is adopted in this study:

$$E(G,h)=\sum_{\eta=0}^{N}\left(y(\eta t_s)-\tilde{y}(\eta t_s)\right)^2 \tag{4}$$

Note that the objective function in (4) is based on the sum of quadratic error, which has been widely used in many literature [28]-[29]. Finally, our problem formulation can be described as follows.

Problem 1. Based on the given real experimental data ($u(t)$, $y(t)$) in figure 1, find the nonlinear function $h(u)$ and the transfer function $G(s)$ such that the objective function in (4) is minimized.

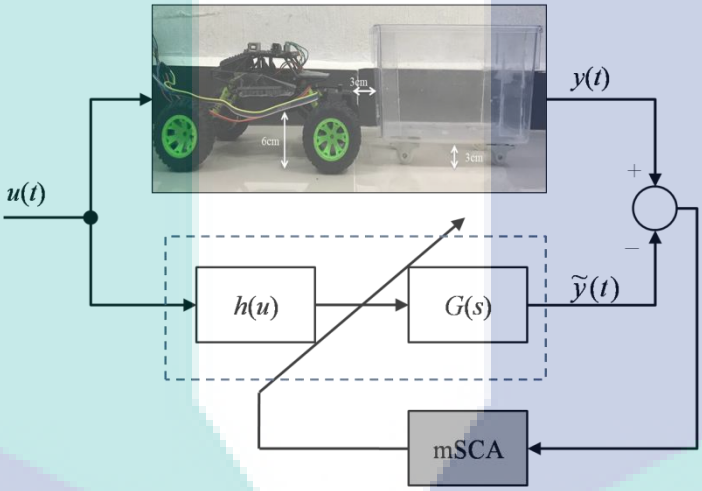

Figure 5. Block diagram of Hammerstein model based mSCA

Furthermore, it is shown on how to apply the SCA in solving **Problem 1**. For simplicity, let the design parameter of **Problem 1** is defined as $\boldsymbol{x}=[b_0\ \ b_1\ \ \cdots\ \ b_{m-1}\ \ a_0\ \ a_1\ \ \cdots\ \ a_m\ \ c_0\ \ \cdots\ \ c_\sigma]^{\mathrm{T}}$, where the elements of the design parameter are the coefficients of both the nonlinear function and the transfer function of the continuous-time Hammerstein model. In SCA framework, let $\boldsymbol{x}_i\ (i=1,2,...,M)$ be the design parameter of each agent i for M total number of agents. Then, consider $x_{ij}\ (j=1,2,...,D)$ be the j-th element of the vector $\boldsymbol{x}_i\ (i=1,2,...,M)$, where D is the size of the design parameter. Thence, by adopting objective function in (4), a minimization problem is expressed as

$$arg \min_{\boldsymbol{x}_i(1),\ \boldsymbol{x}_i(2),...} E(\boldsymbol{x}_i(k)) \tag{5}$$

for iterations k = 1, 2, …, until maximum iteration $k_{\max}$. Finally, the procedure of the mSCA in solving **Problem 1** is shown as follows:

Step 1: Determine the total number of agents M and the maximum iteration $k_{\max}$. Set k = 0 and initialize the design parameter $\boldsymbol{x}_i(0)(i=1,2,...,M)$ according to the upper bound $\boldsymbol{x}_{\text{up}}$ and lower bound $\boldsymbol{x}_{\text{low}}$ values of the design parameter.

Step 2: Calculate the objective function in (4) for each search agent i.

Step 3: Update the values of the best design parameter ***P*** based on the generated objective function in **Step 2**.

Step 4: For each agent, update the design parameter using the following equation:

$$x_{ij}(k+1)=\begin{cases}\dfrac{x_{ij}(k)+P_j}{2}+r_1\sin(r_2)\times\left\|r_3P_j-x_{ij}(k)\right\| & \text{if} \quad r_4<0.5,\\ \dfrac{x_{ij}(k)+P_j}{2}+r_1\cos(r_2)\times\left\|r_3P_j-x_{ij}(k)\right\| & \text{if} \quad r_4\geq 0.5,\end{cases} \tag{6}$$

where

$$r_1=2\left(1-\left(\frac{k}{k_{\max}}\right)^{\alpha}\right)^{\gamma} \tag{7}$$

for maximum iteration $k_{\max}$. In (7), the symbols α and γ are the positive constant values that are introduced to regulate the portion of exploration and exploitation during the tuning process. Note that r_2, r_3 and r_4 are random values that are generated independently and uniformly in the ranges [0, 2π], [0, 2] and [0, 1], respectively. The detailed justification on the selection of the coefficients r_1, r_2, r_3 and r_4 are clearly explained in [26]-[27]. In (6), the symbol $P_j(j = 1, 2, ..., n)$ is denoted as the best current design parameter in j-th element of ***P*** that is kept during tuning process.

Step 5: After the maximum iteration is achieved, record the best design parameter ***P*** and obtained the continuous-time Hammerstein model in figure 1. Otherwise, repeat **Step 2**.

4. Results and Analysis

In this section, the effectiveness of the modified SCA based method for identifying the liquid slosh system using continuous-time Hammerstein model is demonstrated. In particular, the convergence curve response of the objective function in (4), the pole-zero mapping of linear function and the plot of nonlinear function, will be presented and analyzed in this study.

Based on the experimental setup in Section 2, the input response $u(t)$ as shown in figure 3 is applied to the liquid slosh plant, and the output response $y(t)$ is recorded as shown in figure 4. Here, the input and output data are sampled at t_s = 0.02 s for N = 450. In this study, the structure of $G(s)$ is selected as follows:

$$G(s)=\frac{B(s)}{A(s)}=\frac{s^3+b_2s^2+b_1s+b_0}{a_4s^4+a_3s^3+a_2s^2+a_1s+a_0}. \tag{8}$$

after performing several preliminary testing on the given data ($u(t)$, $y(t)$). The fourth order system is used by considering a cascade of 2nd order system for both dc motor of remote car and the slosh dynamic. Meanwhile, the input points for piece-wise affine function of $h(u(t))$ are given by $\boldsymbol{d}$ = [0, 0.2, 0.4, 0.6, 0.8, 1, 2, 3, 4, 5]^T. The selection of vector $\boldsymbol{d}$ is obtained after several preliminary experiments. The design parameter $x \in R^{18}$ with its corresponding transfer function and nonlinear function is shown in Table 1. Next, the mSCA algorithm is applied to tune the design parameter with initial values of design parameter are randomly selected between the upper bound $\boldsymbol{x}_{\text{up}}$ and lower bound $\boldsymbol{x}_{\text{low}}$ as shown in Table 1. Note that the values $\boldsymbol{x}_{\text{up}}$ and $\boldsymbol{x}_{\text{low}}$ are obtained after performing several preliminary experiments. Here, we choose the number of agents M = 40, maximum iterations $k_{\max}$ = 5000, the values α = 0.03 and γ = 0.9.

Figure 6 shows the response of the objective function convergence with the value of $E(G,h)$ = 0.1477 at $k_{\max}$ = 5000 with 82.12 % of objective function improvement to produce the best design parameter ***P***

as shown in the final column of Table 1. It shows that the mSCA based method is able to minimize the objective function in (4) and produce a quite close output response $y(t)$ as compared to the real output $\tilde{y}(t)$, which can be clearly seen in figure 7. Note that the identified output response tends to yield high oscillation when input is injected to the system and it start to attenuate when the input is zero, which is quite similar to the response of real experimental output.

In the real experimental setup, we can say that the liquid slosh system is stable since the liquid slosh output is reduced gradually as $t \to \infty$. In order to validate our model regarding the stability, we use the pole-zero map of the identified transfer function $G(s)$ as shown in figure 8. From the pole-zero map, all the poles are located at the left hand side of y-axis. In particular, the obtained values of poles $-0.0515 \pm j14.2755$, -0.9167 and -3.1230, while the obtained values of zeros are -34.4282 and $-0.2859 \pm j0.4780$. On the other hand, we also can observe the feature of nonlinear function by plotting the obtained piece-wise function as depicted in figure 9. Note that our nonlinear function is not restricted to any form of nonlinear function (i.e., quadratic), which is more generalized and provide more flexibility of searching a justifiable function.

Table 1. Design parameter of liquid slosh plant

$\boldsymbol{x}$	Coefficients	$\boldsymbol{x}_{\text{low}}$	$\boldsymbol{x}_{\text{up}}$	$\boldsymbol{P}$
x_1	b_2	–5	35	35.0000
x_2	b_1	–5	35	19.9949
x_3	b_0	–5	35	10.6786
x_4	a_4	–5	35	–2.2643
x_5	a_3	–2200	–1	–9.3801
x_5	a_2	–2200	–1	–468.8715
x_7	a_1	–2200	–1	–1864.7569
x_8	a_0	–2200	–1	–1321.0211
x_9	c_0	–5	5	1.2708
x_{10}	c_1	–5	5	–0.5736
x_{11}	c_2	–5	5	1.2831
x_{12}	c_3	–5	5	–3.3464
x_{13}	c_4	–5	5	0.9364
x_{14}	c_5	–5	5	–4.2235
x_{15}	c_6	–5	5	–1.3499
x_{16}	c_7	–5	5	–2.6970
x_{17}	c_8	–5	5	–3.5508
x_{18}	c_9	–5	5	4.5195

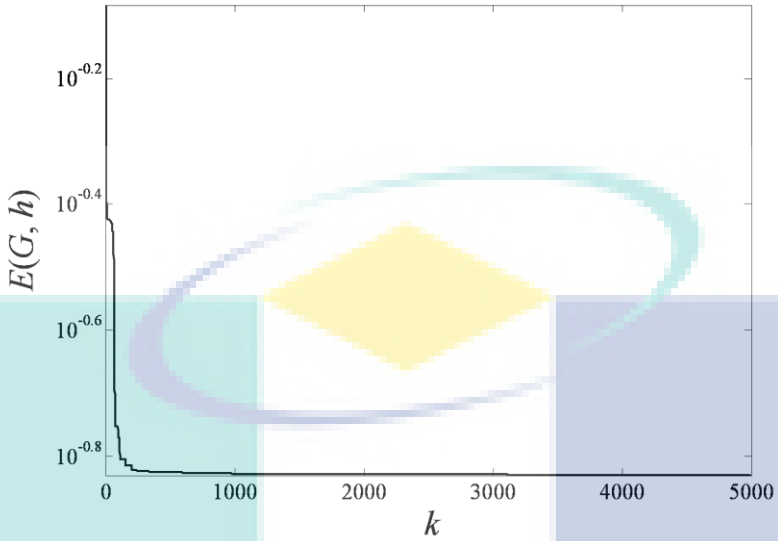

Figure 6. Convergence curve response

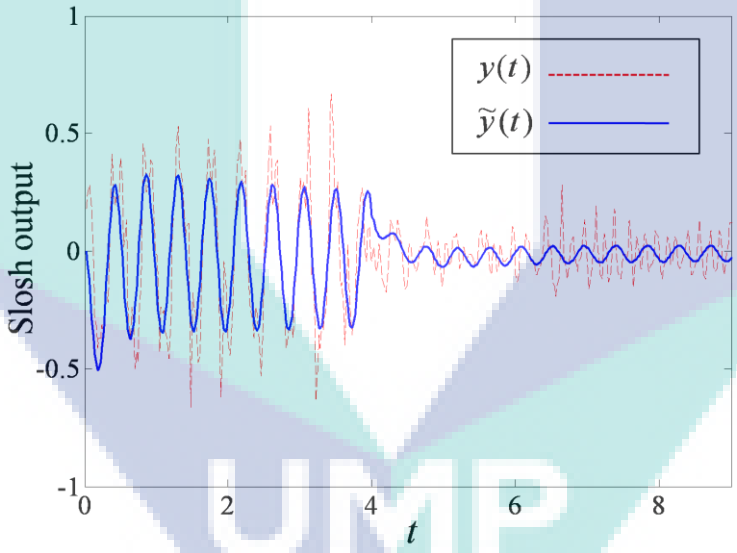

Figure 7. Response of the identified output $\tilde{y}(t)$ and real output $y(t)$

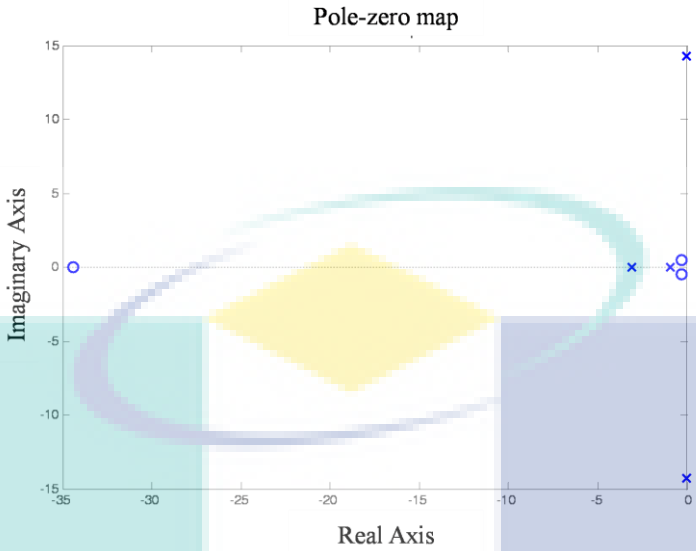

Figure 8. Pole-zero map of transfer function $G(s)$

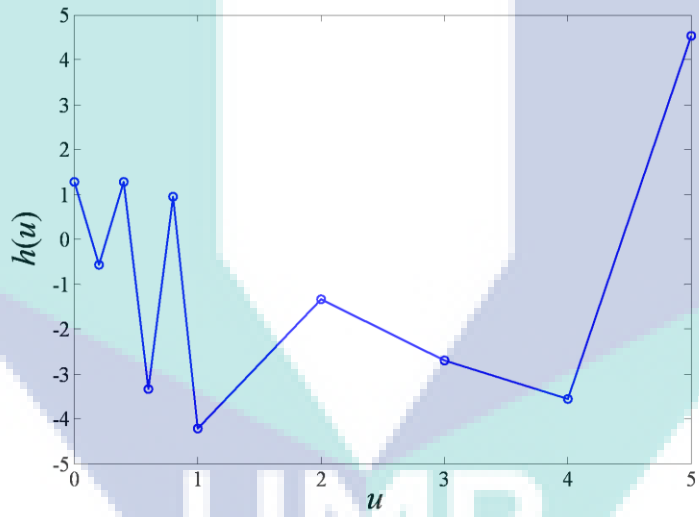

Figure 9. Resultant of piece-wise affine function $h(u)$

5. Conclusion

In this paper, an identification of liquid slosh plant using continuous-time Hammer-stein model based on modified Sine Cosine Algorithm (mSCA) has been presented. The results demonstrated that the proposed generic Hammerstein model based on mSCA has a good potential in identifying the real liquid slosh behavior. In particular, it is shown that the proposed method is able to produce a quite close identified output with real liquid slosh output. Moreover, the resultant linear model has been proved to be stable based on the pole-zero map. It is also shown that the used of piecewise-affine function gives more flexibility for the mSCA to search more generic nonlinear function. In the future, our work can be extended to various types of nonlinear function such as continuous-time Wiener and Hammerstein-Wiener.

Acknowledgments

The authors gratefully acknowledged Research and Innovation Department of Universiti Malaysia Pahang under grant RDU1703153 for the financial support.

References

[1] Rizzuto E and Tedeschi R 1997 Surveys of actual sloshing loads on board of ships at sea *Proc. of Int. Conf. on Ship and Marine Research* p 7.29-7.37.

[2] Terashima K and Schmidt G 1994 Sloshing analysis and suppression control of tilting-type automatic pouring machine *Proc. of IEEE Int. Symp. on Industrial Electronics* p 275-280.

[3] Acarman T and Ozguner U 2006 Rollover prevention for heavy trucks using frequency shaped sliding mode control *Vehicle System Dynamics* vol 44(10) p 737-762.

[4] Li C, Zhu X, Cao G, Sui S and Hu M 2008 Identification of the Hammerstein model of a PEMFC stack based on least squares support vector machines *J. of Power Sources*vol 175 p 303-316.

[5] Kara T and Eker I 2004 Nonlinear modeling and identification of a DC motor for bidirectional operation with real time experiments *Energy Conversion and Management* vol 45(7-8) p 1087-1106.

[6] Su SW, Wang L, Celler BG and Savkin AV 2007 Oxygen uptake estimation in humans during exercise using a Hammerstein model *Annals of biomedical engineering*vol35(11) p 1898-1906.

[7] Westwick DT and Kearney RE 2001 Separable least squares identification of nonlinear Hammerstein models: Application to stretch reflex dynamics. *Annals of Biomedical Engineering* vol 29(8) p 707-718.

[8] Zhang Q, Wang Q and Li G 2016 Nonlinear modeling and predictive functional control of Hammerstein system with application to the turntable servo system *Mechanical Systems and Signal Processing* vol 72 p 383-394.

[9] Ai Q, Peng Y, Zuo J, Meng W and Liu Q 2019 Hammerstein model for hysteresis characteristics of pneumatic muscle actuators. *Int. J. of Intelligent Robotics and Applications* vol 3(1) p 33-44.

[10] Saleem A, Mesbah M and Al-Ratout S 2017 Nonlinear Hammerstein model identification of amplified piezoelectric actuators (APAs): Experimental considerations *4th Int. Conf. on Control, Decision and Information Technologies* p 0633-0638.

[11] Zhang HT, Hu B, Li L, Chen Z, Wu D, Xu B, Huang X, Gu G and Yuan Y 2018 Distributed Hammerstein Modeling for Cross-Coupling Effect of Multiaxis Piezoelectric Micropositioning Stages*IEEE/ASME Transactions on Mechatronics* vol 23(6) p 2794-2804.

[12] Bai EW and Li D 2004 Convergence of the iterative Hammerstein system identification algorithm *IEEE Transactions on automatic control* vol 49(11) p 1929-1940.

[13] Hou J, Chen F, Li P and Zhu Z 2019 Fixed point iteration-based subspace identification of Hammerstein state-space models *IET Control Theory & Applications* vol 13(8) p 1173-1181.

[14] Ge Z, Ding F, Xu L, Alsaedi A and Hayat T 2019 Gradient-based iterative identification method for multivariate equation-error autoregressive moving average systems using the decomposition technique *J. of the Franklin Institute* vol 356(3) p 1658-1676.

[15] HouJ, Liu T, Wahlberg B and Jansson M 2018 Subspace Hammerstein model identification under periodic disturbance *IFAC-PapersOnLine* vol 51(15) p 335-340.

[16] Hou J, Liu T and Wang QG 2019 Subspace identification of Hammerstein-type nonlinear systems subject to unknown periodic disturbance. *Int. J. of Control, (just-accepted)* p 1-29.

[17] Jamaludin IW and Wahab NA 2017 Recursive Subspace Identification Algorithm using the Propagator Based Method *Indonesian J. of Electrical Engineering and Computer Science* vol 6(1) p 172-179.

[18] Wang D and Zhang W2015 Improved least squares identification algorithm for multivariable Hammerstein systems *J. of the Franklin Institute* vol 352(11) p 5292-5307.

[19] Bai EW 2002 A blind approach to the Hammerstein–Wiener model identification *Automatica* vol 38(6) p 967-979.

[20] Ma L and Liu X 2015 A nonlinear recursive instrumental variables identification method of Hammerstein ARMAX system. *Nonlinear Dynamics* vol 79(2) p 1601-1613.

[21] Lin W and Liu PX 2006 Hammerstein model identification based on bacterial foraging *Electronics Letters* vol 42(23) p 1332-1333.

[22] Gotmare A, Patidar R and George NV 2015 Nonlinear system identification using a cuckoo search optimized adaptive Hammerstein model *Expert systems with applications* vol 42(5) p 2538-2546.
[23] Al-Duwaish HN 2011 Identification of Hammerstein models with known nonlinearity structure using particle swarm optimization *Arabian J. for Science and Engineering* vol 36(7) p 1269-1276.
[24] Zhang H and Zhang H 2013 Identification of Hammerstein Model Based on Quantum Genetic Algorithm *Telkomnika* vol 11(12) p 7206-7212.
[25] Mirjalili S 2016 SCA: a sine cosine algorithm for solving optimization problems. *Knowledge-Based Systems* vol 96 p 120-133.
[26] Suid MH, Tumari MZ and Ahmad MA 2019 A modified sine cosine algorithm for improving wind plant energy production. *Indonesian J. of Electrical Engineering and Computer Science* vol 16(1) p 101-106.
[27] Suid MH, Ahmad MA, Ismail MRTR, Ghazali MR, Irawan A and Tumari MZ 2018 An Improved Sine Cosine Algorithm for Solving Optimization Problems *IEEE Conf. on Systems, Process and Control* p 209-213.
[28] Mjahed M. and Ayad H 2019 Quadrotor Identification through the Cooperative Particle Swarm Optimization-Cuckoo Search Approach. *Computational intelligence and neuroscience*p 1-10.
[29] Gupta S, Gupta R and Padhee S 2018 Parametric system identification and robust controller design for liquid–liquid heat exchanger system *IET Control Theory & Applications* vol 12(10) p 1474-1482.